5-5-2020

A DOE to Determine Significant Manufacturing Parameters for OPV Devices

Iain Tracton
ixt5396@rit.edu

RIT

A DOE to Determine Significant Manufacturing Parameters for OPV Devices

By Iain Tracton

A Thesis Submitted in Partial Fulfillment of the Requirements for the Degree of Master of Science in Mechanical Engineering

Department of Mechanical Engineering, Kate Gleason Collage of Engineering, Rochester Institute of Technology (RIT)

Rochester Institute of Technology
Rochester, NY
May 5, 2020

Committee Approval

_____

Dr. Chris Collison, *Thesis Advisor* Date

_____

Dr. Rob Stevens, *Committee Member* Date

_____

Dr. Scott Williams, *Committee Member* Date

_____

Dr. Michael Schlau, *Department Representative, Graduate Director* Date

Abstract

The study of alternative energy sources is important to fighting climate change by reducing our dependence on burning of fossil fuels. Solar power is of interest because of the immense power radiated by the sun. Organic Photovoltaic (OPV) devices offer the ability to produce cheaper solar power but are challenged by low device efficiencies. In this study we work with devices made from squaraines (SQ) and a common functionalized fullerene (PCBM). We conduct a Design of Experiments (DOE) to determine what manufacturing parameters are affecting device efficiencies. By conducting a DOE, we also gain the ability to determine if there are significant interactions between parameters that are affecting device efficiencies. The parameters chosen (and levels) for investigation were the blend ratio (SQ:PCBM of 3:7 and 1:3), solvent additive (Tetrahydrofuran (THF) and Dimethyl Acetamide (DMA)), concentration of casting solution (12mg/mL and 16mg/mL), spin speed (1200rpm and 1600rpm), annealing time (5mins and 15mins), and annealing temperature (90°C and 120°C). Chloroform served as the main solvent in an 85:15 volume ratio with the additive. Despite an incomplete data set, we were able to determine that the solvent additive (sometimes referred to as a co-solvent) significantly affects device performance: none of the devices made with DMA worked. The cause of this appears to be to have been significant phase separation of our squaraine electron donor and functionalized fullerene acceptor. This paper also critiques the use of DOEs as a research technique and advocates for their use in OPVs because they provide a rigorous and robust methodology for the study of OPVs while also screening variables and interactions for which ones will drive predictive models of device performance, and moving us toward processes that are robust enough to be scaled up when it is becomes time to bring OPVs to market

Acknowledgements

To Shirley Tracton – It's Done

Dr. Chris Collison – For being willing to work with a mechanical engineering student that he had never met before on a crazy idea.

Dr. Scott Williams – For pointing me towards Dr. Collison.

Dr. Rob Stevens – For patience and support.

Dr.s Schrlau and Crassidis – For believing I could make it in the MS program and guiding me when I doubted myself.

Matt Seitz and Tyler Wiegand – For being superfluous co-conspirators, commiserators, and detectives.

Soumya Gupta – For my crash course in all thing's lab related as well as supporting me in my efforts.

Chenyu Zheng – For a record of excellence, and a body of research I relied heavily upon.

The Remainder of the Collison Lab Group (2018 – 2020) – For being ever curious and willing to help.

The Cody Lab Group – For being suppliers of the highest quality.

Michael Grant – For liaising between groups and support.

Kerri Bondi and Kathy Reid – For truly unending support throughout my time at RIT and curating the community that was my home.

Sam Tracton – For the humor and brotherly love that I always rely on

Debra and Keith Tracton - For being loving and supporting parents that have never cared about anything more than me and Sam

And the rest of my family and friends for your love, support, and time…

Table of Contents

Committee Approval ii

Abstract iii

Acknowledgements iv

Table of Contents v

List of Figures vii

List of Tables viii

List of Equations ix

Introduction 1

What is a Design of Experiments (DOE)? 4

Review of How DOEs Add Value to the Analysis of Complex Systems 6

Experimental Background and Design 8

- Absorption 10
- Exciton Diffusion 11
- Charge Transfer 12
- Charge Dissociation 13
- Aggregation, Device Microstructure, and Device Performance: A Summary 13
- Experimental Details 14

Experimental Procedure 22

- DOE Structure and Order of Experiments 22
- Materials 22
- PCBM Acceptance 23
- Device Manufacture 23
- ITO Etching 23
- Substrate Cleaning 24
- MoO_3 Deposition 24
- Solution Preparation and Spin Coating 25
- Annealing 26

Aluminum Deposition 26
Spectroscopy Samples 26
Performance Testing 27
UV-Vis Spectroscopy 28
SEM Imagining 28
Metrics 29
DOE Results 32
Analysis 34
Conclusion 39
Appendix I: Table of Individual Trial Specifications 43
Appendix II: NREL Statement 46
References 47

List of Figures

Figure 1: Graph depicting the different types of photovoltaic devices and how the efficiency of each type has increased over time. OPV devices reside in the lower right-hand corner. The chart "Best Research-Cell Efficiencies" is reprinted with permission from the National Renewable Energy Laboratory, https://www.nrel.gov/pv/assets/images/efficiency-chart.png, Accessed June 13, 2018 [5] 1
Figure 2: Diagram of the layered structure of our devices. 9
Figure 3: Depiction of the mixed nature of a bulk heterojunction (BHJ). 9
Figure 4: Depiction of the Photon to Electron Conversion Process. Roman numerals next to efficiency labels indicate the step. I: Absorption, II: Exciton Diffusion, III: Charge Transfer, IV: Charge Dissociation. Dashed black lines indicate charge carrier movements and transitions, while dashed orange lines indicate binding of two charge carriers. 10
Figure 5: Normalized UV-Vis absorption spectra of DBSQ(OH)2 in solution and as a thin film. 11
Figure 6: The basic structure of a squaraine. For DBSQ(OH)2 the R groups are butyl groups. .. 11
Figure 7: Graph of a hypothetical JV curve produced by a hypothetical OPV device (not to scale with what our devices produced) while illuminated The Voc and Jsc are labeled and an attempt is made to depict the FF(the ratio of the actual maximum power to theoretical max power). 30
Figure 8: SEM images active layers as they appear on spectroscopy slides. THF was used as the solvent additive (left). DMA was used as the solvent additive (right). 35
Figure 9: Graph of the composite minimum and maximum spectra by the solvent additive used. "Composite" indicates that each data point is the maximum or minimum (depending on which spectrum is looked at) absorbance for a given wavelength of all devices made with the indicated solvent additive. 36

List of Tables

Table 1: Table of factors and high- and low-level values. 15
Table 2: Table of factors and what aspect of a device's microstructure they effect (along with the device process or property). 17
Table 3: Table of factors, the trials that were run and their results. The bright green highlighted PCE value is the highest value, 2.5%. This is within the typical range of efficiencies for DBSQ(OH)2. The faded green FF values are > 45%, which represents an el elevated FF from what is typically seen. The faded green Jsc values are <-7 mA while the faded red values are >-1mA (as more negative current is desired). The faded green Voc values are >0.7V and the faded red values are >0.1V. The bright red failure rate values are > 66.67%. 33
Table 4: Table of average PCE values of devices produced at different annealing condition and the weighted standard deviation of the average PCE across multiple trials with the same annealing conditions. 37
Table 5: Table of average PCE values of devices produced using different blend ratios and the weighted standard deviation of the average PCE across multiple trials with the same blend ratio. 37
Table 6: Table of device performance parameters (as weighted averages) and their associated weighted standard deviation. 38

List of Equations

Equation 1: Number of Trials in a DOE 5
Equation 2: Calculation of PCE from measured parameters 29

Introduction

It is well known that global warming and climate change are cause for concern. The leading cause of global warming is the release of Carbon Dioxide (CO_2) and other "greenhouse gases" into the environment. The generation of power by burning fossil fuels is the main source of greenhouse gasses released into the environment. To reduce greenhouse gas emissions, many types of alternative power generation have been developed, including wind power, hydropower, and solar power.

Solar power is of greatest interest because the amount of energy the sun radiates is many times what is required to furnish the needs of the planet. This contrasts with fossil fuels which will only become more scarce and harder to access with time. The question then, is how to harness the immense amount of solar energy that is available.

There are many answers to this question. Figure 1 illustrates the breadth of types of solar cells and how their efficiencies have improved over time. Solar cells, or devices, which are described in Figure 1 can be grouped into two main categories: inorganic and organic devices. Inorganic devices use main group semiconductors to absorb light and separate charges, while organic devices use, specifically, carbon-based materials. As can be seen in Figure 1, inorganic devices are generally more efficient than organic devices. However, inorganic devices are typically fragile, hard to manufacture, and expensive [1–4]. Since organic materials can be very

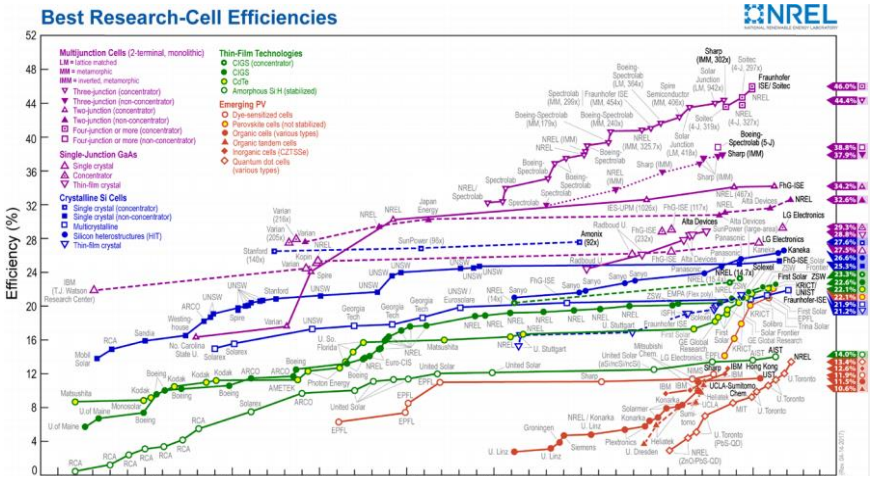

Figure 1: Graph depicting the different types of photovoltaic devices and how the efficiency of each type has increased over time. OPV devices reside in the lower right-hand corner. The chart "Best Research-Cell Efficiencies" is reprinted with permission from the National Renewable Energy Laboratory, https://www.nrel.gov/pv/assets/images/efficiency-chart.png, Accessed June 13, 2018 [5]

flexible, comparatively easy to work with, inexpensive, and can be designed on a molecular level, there is hope that they will prove to be a solution towards bringing solar-powered devices into the everyday.

There are, of course, challenges to reducing the cost per kilowatt-hour of power produced by organic photovoltaic (OPV) devices. The first challenge is the low efficiency of OPV devices. Upscaling manufacturing processes to industrial levels is the second challenge. These challenges include solvent and material handling, environmental controls, designing robust manufacturing equipment and techniques, and a host of other process dependent details that could possibly increase the complexity of scaling up manufacturing [5–9]. Both sets of challenges are critical to the acceptance and use of OPV devices, because acceptance will require not only efficient devices but efficient and safe manufacturing processes. This leads to the conclusion that the process of making OPV devices is just as important to the success of the technology as the materials used to make the devices themselves.

The goal of this work was to determine what manufacturing parameters had a significant effect on device performance. The secondary objective of this work was to determine what manufacturing parameters had a significant effect on the process yield. To do this, we attempted a 6 factor (parameter), 2 level (values experimented at), full factorial design of experiments (DOE). The factors/parameters of interest were blend ratio, solvent additive, concentration of the casting solution, spin speed of the spin coater, and annealing time and temperature. Specifically, we were interested in how changes to these parameters affect power conversion efficiency (PCE), fill factor (FF), open circuit voltage (Voc), short circuit current density (Jsc), and device failure rate. PCE, FF, Voc, and Jsc are all standard metrics for determining device performance. The device failure rate was used to analyze which manufacturing parameters influenced process yield.

Determining the significance of manufacturing parameters is important to the larger challenges facing OPVs because it not only allows us to learn what parameters to focus on when optimizing devices, but also helps to characterize which interaction paradigms control the microstructure of a device. The hope is that this work, along with future work, can optimize parameters for the different types of materials used to make OPV devices and provide the experience and knowledge necessary to scale production to industrial levels without setbacks. The ultimate goal of this work is to determine the assembly paradigms of $DBSQ(OH)_2$:$PC_{61}BM$

films and to model how they are affected by manufacturing parameters to work towards the construction of a more general model for optimizing OPV devices based on the donor and acceptor selected.

What is a Design of Experiments (DOE)?

A DOE is a statistical analysis technique where factors (variables/parameters) are varied randomly between fixed levels (quantitative or qualitative set points). The number of trials that must be performed is given by Equation 1, where L is the number of levels, F is the number of factors, and k is a nonnegative integer < F which dictates the resolution of the DOE. The resolution of a design indicates the level of interaction between factors that the DOE can identify the effect and significance of. Interactions are considered to have an effect when the resulting outcome is different from the sum of the effects of the factors [10]. We chose to conduct a full factorial design, meaning that we selected $k = 0$, so the significance of *all* interactions between factors can be isolated and determined.

Choosing k > 0 reduces the resolution of the design, causing main effects (the effects caused solely by factors) and lower order interactions (the interactions of 2 and sometimes 3 factors) to become confounded with the higher order interactions (the interactions of 3 or more factors). Given the size of our design, it would not have been unreasonable to choose k=1, because it is generally considered "safe" to assume that the higher order interactions are insignificant and so neglect any effect they may have, thus we could have determined the significance of our main effects and first order interactions (interactions of 2 factors, which are assumed to be the most likely to occur) while conducting less experiments then we did. The larger k is chosen to be, the lower the order of the interactions that are confounded with the main effects and with the first order interactions, reducing the likelihood significance will be determined correctly. Given the size of our design, selecting k>1 would have been unreasonable because the order of the interactions confounded with our main effects and first order interactions would have been too low [11]. However, we selected k=0 because we could not find an analysis in the literature that varied multiple factors at once; leaving us with no indication, other than statistical intuition, that our higher order interactions would be insignificant. The cost, of course, is that our design requires 64 trials.

When complete, the analysis yields the significance of parameters and interactions to each output, the best "recipe" of the trials, and trends for how each output varies with each factor. In a 2-level design, like we have conducted, the trends that will result *will* be linear regardless of the shape of the real trend. This may be an important limitation when developing a

model. The other results can be used to optimize the manufacturing process for high output and/or (depending on the nature of the trends) allows devices to be optimized for efficiency, current, or voltage depending on the application of the devices. The significance data can be used to determine which parameters to focus further study (and possibly optimization) on, since these will be the parameters and interactions which control the assembly of the active layer microstructure.

$$N = L^{(F-k)}, k = nonnegative\ integer < F \quad (1)$$

Review of How DOEs Add Value to the Analysis of Complex Systems

Our primary reason for conducting a DOE was that DOEs can determine the significance and effect of interactions between factors. Many design parameters, including those used to design the materials themselves and the manufacturing process, have been studied extensively in One Variable At-a-Time (OVAT) setups. Inherent in an OVAT style analysis is the assumption that the different variables that could be manipulated do not interact [12]. We wanted to relax that assumption and study the interactions between variables. Additionally, the manner in which DOEs are conducted reduces the number of trials required to analyze complex systems and helps to remove noise and bias from systems that are hard to control.

One of the primary features of a DOE is a randomized run order. The run order is the order in which individual trials are conducted (our runs were conducted in the order they appear in Appendix I). The randomization of the run order is important because it helps to dampen out the effects of uncontrolled variables, called noise variables. The noise variables primarily arise from things that could change in our experimental process as time passes (trial to trial, daily, or seasonally) and are not specifically controlled [10,13]. Examples of noise variables in our study include the ambient temperature and humidity in our glove boxes, the number of times the evaporations boats have been used, the amount of material in the evaporation boats, the time the solutions are held before casting, the time between casting and annealing, how well our probes made electrical contact with the devices being tested. It is important that noise variables are appropriately dampened so that they do not cause us to see false effects or significance [10,13].

It is common for texts discussing DOEs to highlight their ability to reduce the number of trials required to analyze a system when compared to an OVAT analysis [10,12]. However, this can be invalidated by increasing the number of levels that factors are tested at by too much (which may be necessary if a more detailed response model is required). Zhu et al. conducted a study in 2018 on improving charge carrier transport in squaraine based organic solar cells which can be used to highlight how using a DOE can reduce the number of trials run in a study. In their study Zhu et al. tested ternary devices to show how adding a second donor material can improve device performance (specifically by improving charge carrier mobility, thus increasing Jsc and PCE). This is done by testing devices with different blend ratios, a factor we were also interested in [14]. In our study we conceptualize the blend ratio as one factor but for Zhu et al. it should be

considered as two factors, one for the weight percent of each donor. Both donors are varied from zero parts to 1 part. LQ-51 (Donor 1) is held at 1 part except for one trial where it is set to 0, and PCDTBT (Donor 2) is trialed at 0, 0.1, 0.3, 0.5, 0.7, and 1 part. All told there are 7 trials conducted [14]. If this was formulated as a DOE it could be done as a 2 factor, 2 level, full factorial design which only requires 4 trials (it would actually be 3 trials in this case because when both donors are set to 0 a working device cannot be made). The factors are Donor 1 and Donor 2, and the levels would be either 0 or 1 part. Since the goal is to find evidence of increased charge mobility in the ternary device a smaller gradient of levels is unnecessary.

Additional examples of how DOEs reduce the number of trials required by a study can be drawn from our own lab. In his 2019 dissertation Zheng conducts on optimization of devices made with $DBSQ(OH)_2$, $DPSQ(OH)_2$, and $DHSQ(OH)_2$. First, Zheng makes devices at 6 different blend ratios of squaraine and $PC_{61}BM$ (18 trials). Then the blend ratio which performed the best are remade using $PC_{71}BM$ as the acceptor (3 trials, 21 trials total) [15]. This can be reduced using what is known as a mixed level or asymmetric design, a type of DOE where groups of factors are trialed at different numbers of levels, to 18 total trials [16,17]. In this case the factors are the donor material side chain length, the acceptor material base fullerene size/shape, and the blend ratio. The fullerene size/shape is trialed at two levels while the donor and blend ratio are trialed at three levels. It is appropriate to reduce the number of levels from the 6 done by Zheng to 3 because three levels are still enough to capture general nonlinearity in the response [10,11,15].

Conducting Zheng's experiments as a DOE would have had the added benefit of trialing all three donors at all three blend ratios with $PC_{71}BM$, something Zheng does not do. The improved PCE and Jsc seen in devices made with $PC_{71}BM$ is attributed to its broader absorbance spectrum, compared to $PC_{61}BM$ [15]. However, by simply taking the best performing $PC_{61}BM$ devices and changing the acceptor to $PC_{71}BM$ Zheng essentially assumes that the materials will otherwise behave the same (i.e. that there will be no statistical interaction between the donor and the acceptor). Conducting a DOE would have allowed for the investigation of this as a hypothesis, rather than requiring an assumption to be made. By eliminating assumptions and reducing the number of trials required for a study, DOEs allow us to conduct more thorough and efficient experiments.

Experimental Background and Design

The goal of this section is to detail sufficient background about OPV for the reader to understand, at a high level, how and why they work. Additionally, this section will detail the actual experiment conducted, and the reader should understand that the parameters/factors affect the microstructure of an OPV device. First, an overview of OPV device structure will be given and the primary mechanisms of OPV will be discussed. These mechanisms are absorption, exciton diffusion, charge transfer, and charge dissociation

The OPV devices made in our lab have 6 layers; soda lime float glass, indium tin oxide (ITO), molybdenum (IV) oxide (MoO_3), the active layer, and aluminum. The soda lime float glass is the bottom of a device, as shown in Figure 2, and allows light to pass into the device. Float glass is used in our lab because of its superior flatness compared to glass manufactured by other techniques. Flatter glass allows for a more even spin coating of the layers onto the device. ITO is used as the transparent electrode. MoO_3 serves as a hole transport layer. A hole transport layer is a layer through which only free charge carriers (free electrons or free "holes") with positive charge (free holes) may move. This causes devices to have distinct positive and negative electrodes, as well as to behave like diodes, which is useful during performance measurement because it means that important metrics can be seen on the current-voltage graph of an operating device that is exposed to a range of voltages. Additionally, the hole transport layer increases device power conversion efficiency (PCE), the usual metric by which devices are compared, because it reduces the recombination of free charge carriers as they move to the electrodes by preventing them from moving in the same direction through the device [18–20]. The active layer is the layer of the device that absorbs light and produces free charge carriers. We spin cast this layer from a solution of the electron donating (donor) material, electron accepting (acceptor) material, and an organic solvent, usually chloroform. The solvent evaporates during spin coating leaving the donor and acceptor material mixed in what is called a bulk heterojunction (BHJ) [15]. This means that within the active layer there are no distinct layers of donor or accepter, as depicted in Figure 3. Instead there are many small domains of each material (and sometimes mixed domains), which help to improve PCE by increasing the likelihood that an excited

particle, called an exciton, can reach the donor-acceptor interface before it relaxes back to the ground state. Lastly, aluminum is evaporated onto the devices to serve as the second electrode.

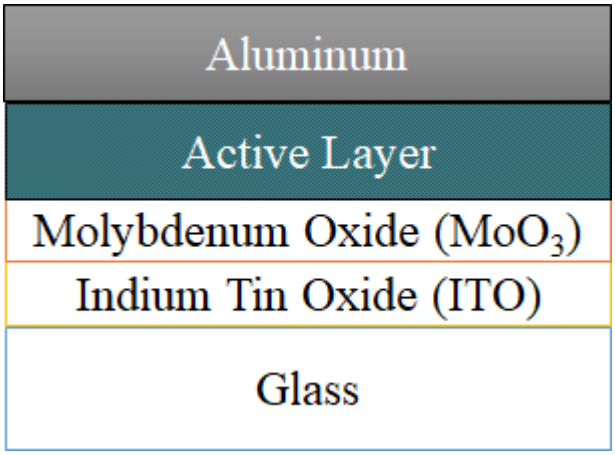

Figure 2: Diagram of the layered structure of our devices.

Figure 3: Depiction of the mixed nature of a bulk heterojunction (BHJ).

There are four major processes or steps in photon to electron conversion. The first is absorption, where a photon is absorbed by an electron donor (or acceptor) molecule, and an electron is excited in the material, forming an *exciton* (an excited electron-hole pair). The next step is exciton diffusion where the exciton moves to the interface between the electron donor and electron acceptor. Once the exciton is at the donor-acceptor interface charge transfer can occur. In charge transfer the electron, while still bound to the hole inside the neutral photoexcited molecule, moves from the donor to the acceptor, forming a charge transfer state (or a charge transfer exciton). Lastly, charge dissociation occurs. In this step, the charge transfer state is broken down into a free electron and hole. These charge carriers are then free to move to the appropriate electrode [5,12]. Figure 4 provides a visual reference for the whole process.

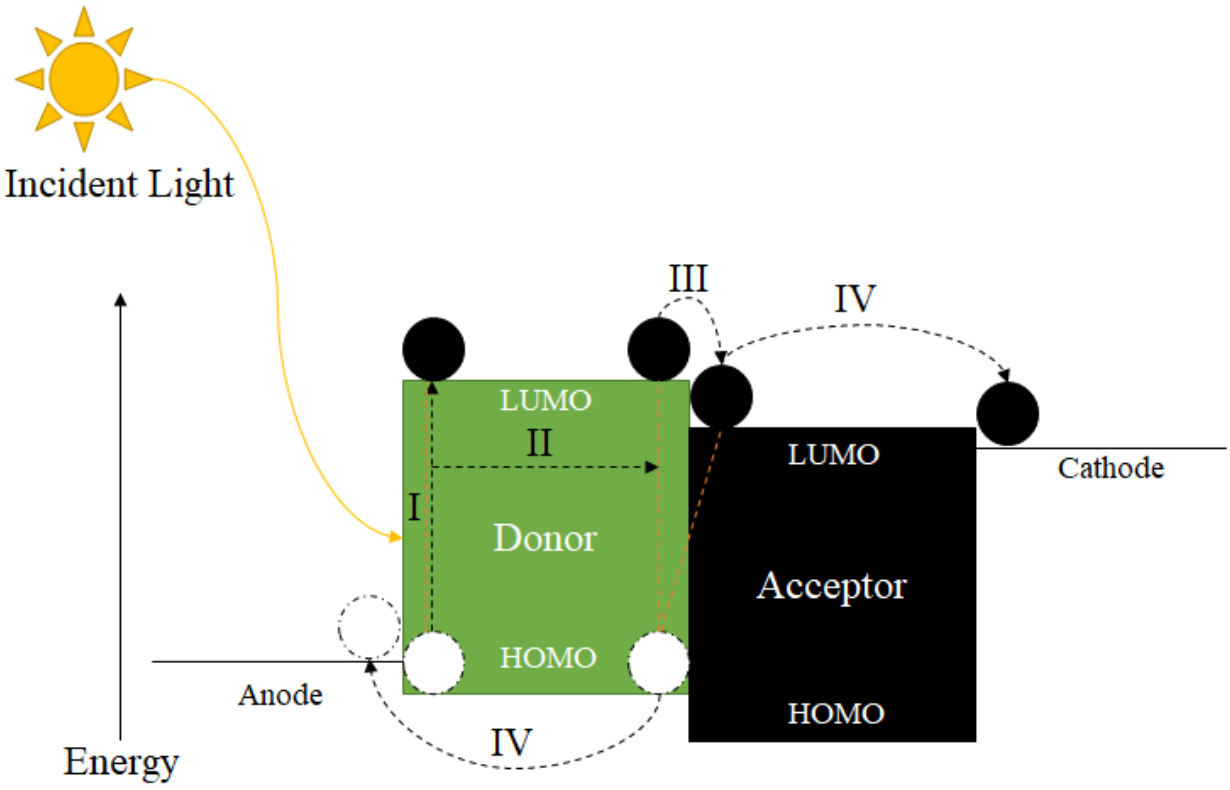

Figure 4: Depiction of the Photon to Electron Conversion Process. Roman numerals next to efficiency labels indicate the step. I: Absorption, II: Exciton Diffusion, III: Charge Transfer, IV: Charge Dissociation. Dashed black lines indicate charge carrier movements and transitions, while dashed orange lines indicate binding of two charge carriers.

Absorption

Absorption is the process by which an incoming, or incident, photon transfers energy to an electron. This causes the electron to move from the highest occupied molecular orbital (HOMO) to the lowest unoccupied molecular orbital (LUMO). Figure 5 shows the absorbance spectrum, taken via ultraviolet-visible (UV-VIS) spectroscopy, of, 2,4- bis-(4-dibutylamino-2,6-dihydroxyphenyl) cyclobutane-1,3-dione ($DBSQ(OH)_2$, the squaraine used in this study) in solution and in a thin film to visualize which wavelengths of light can induce a transition. The structure of squaraines can be seen in Figure 6 (for $DBSQ(OH)_2$ the R groups are butyl groups).The most important feature of Figure 5 is how the absorbance spectrum changes from the solution to the thin film. This happens because the solution spectrum is essentially the spectrum of each isolated molecule, often called a monomer, while the thin film allows for aggregation.

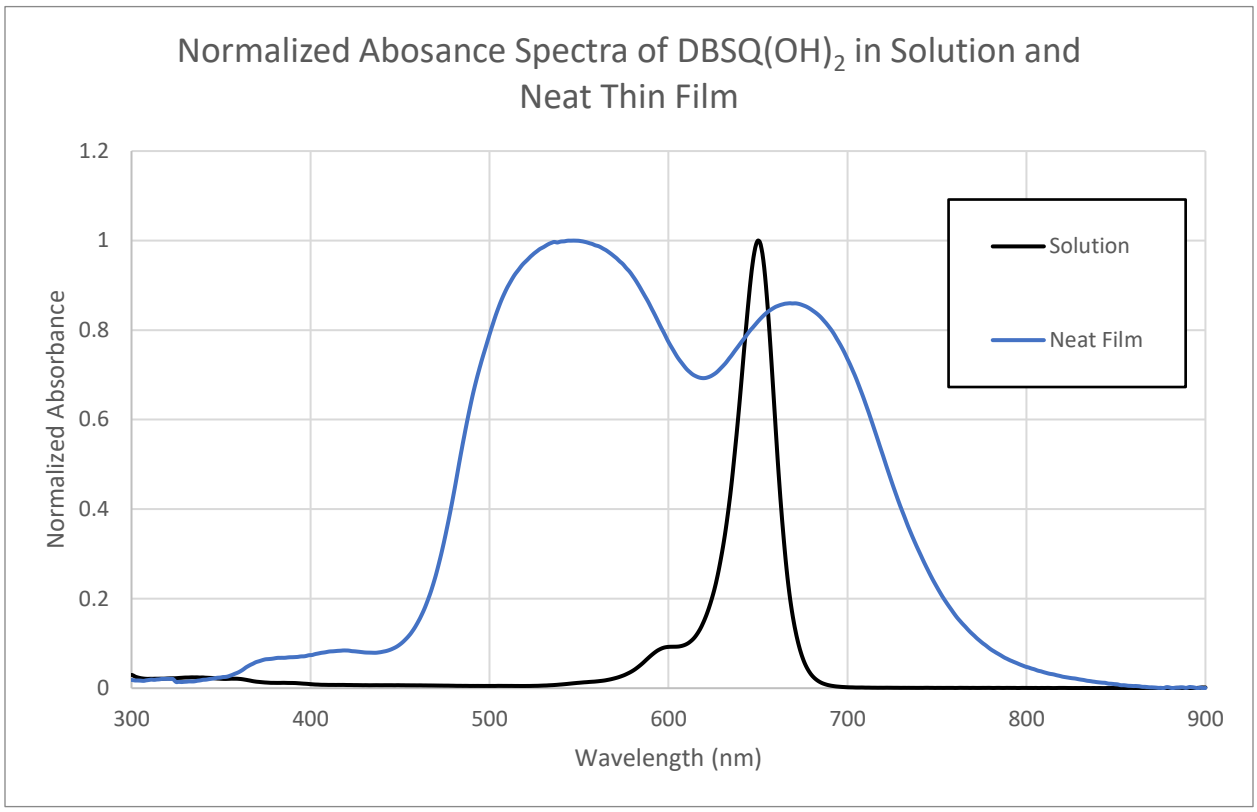

Figure 5: Normalized UV-Vis absorption spectra of DBSQ(OH)2 in solution and as a thin film.

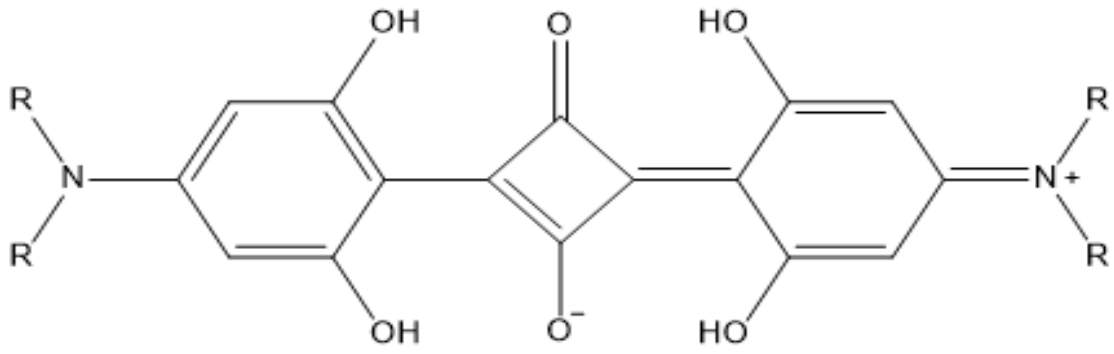

Figure 6: The basic structure of a squaraine. For DBSQ(OH)2 the R groups are butyl groups.

Exciton Diffusion

After absorption, the excited electron-hole pair exists in a coulombically bound state referred to as an exciton which must diffuse from excitation loci to the BHJ, or donor-acceptor, interface. Typically, in an organic semiconductor, an exciton can travel 10 - 20nm before recombination occurs [21,22]. So, domain size, a feature of the device microstructure, is critical for the function of a device.

Charge Transfer

After an exciton reaches the donor-acceptor interface, charge transfer (CT) occurs. The bound electron may move from the electron donor into the electron acceptor, to form a bound charge transfer (CT) state [23]. There is a debate in the literature as to how CT states form [24,25]. Fortunately, despite the lack of consensus on the mechanistic nuances, the efficiency of this step can be near one hundred percent [26].

The OPV community at large has been able to determine empirically that CT is dependent upon the energy offsets and the balance of charge carrier mobilities [27,28]. The energy offset is the difference in the energy of the LUMOs of the donor and acceptor [28]. It is also the energy lost to drive CT and should be designed to be about 0.2eV through careful material selection. If the energy offset is any larger than 0.2eV then there is unnecessary energy loss for little or no gain in efficiency of CT and a possible reduction of device Voc [28]. If the energy offset is any less than 0.2eV, then there can be a drop in efficiency of CT, which will appear as a drop in Jsc and PCE [28].

Charge carrier mobilities refer to the ease with which electrons and holes move through a material. In a binary BHJ device there are four mobilities (the hole mobility in the electron donor, the electron mobility in the electron donor, the hole mobility in the electron acceptor, and the electron mobility in the electron acceptor), however, we typically only care about two; the electron mobility in the electron acceptor material and the hole mobility in the electron donor material. It is important that these two mobilities are balanced because if they are not, a charge bias, which can be thought of as a voltage bias, will build up at the donor-acceptor interface. This will counter the energy offset and reduce the efficiency of charge transfer [15,29].

Charge Dissociation

Charge dissociation is the fourth and final step of the photon to electron conversion process. In this step, the coulombic binding of the exciton is broken, and free charge carriers move to the electrodes. Ultimately, it is the separation of charges that allows a photovoltaic device to produce power. Charge dissociation is affected by the free charge carrier mobilities, the dielectric constants of the donor and acceptor, and the length of the percolation paths [15]. The dielectric constant is the ratio of the electric permittivity of a material to the electric permittivity of a vacuum. The larger this ratio is, the easier it is to separate charges within a material. Ultimately, the dielectric of a device is lower than the dielectric of the external circuit, which causes the free charges to recombine by flowing around the external circuit. The percolation path lengths are the distances that free charge carriers must travel to an electrode and are controlled by the microstructure [15,30].

Aggregation, Device Microstructure, and Device Performance: A Summary

Aggregation covers three phenomena: phase separation, domain crystallinity, and molecular orbital overlap (electronic aggregation). Phase separation and domain crystallinity are descriptions of the physical arrangement of materials and molecules within the device microstructure, while molecular orbital overlap describes the intermolecular interactions between molecules of the same material. The different types of aggregation affect the photon to electron conversion process differently during the different steps leading to changes in device performance.

Absorption is predominantly affected by molecular orbital overlap. The overlapping of the LUMOs of different molecules of the same material causes the associated energy level to split. This change results in some different wavelengths of light absorbing into the material, as compared to the unaggregated material [15,31]. Because electronic aggregation can only happen in homogeneous domains, absorption spectra can also be used to give an indication of the extent of phase separation within a device's microstructure [31,32]. In general, increases in absorption cause increases in the short circuit current density, Jsc, and power conversion efficiency (PCE) by converting more incident photons into excitons [15,22,25]. Electronic aggregation can have

the same effect by allowing the absorption of photons that would normally not be absorbed, however the associated phase separation can reduce the efficiency of the other steps in the photon to electron conversion process limiting the benefit of electronic aggregation [15,32–35].

Exciton diffusion is largely controlled by the domain size, since the excitons have a limited lifetime and must reach the donor-acceptor interface before they relax back to the ground (unexcited) state. The domain size will initially be determined by the miscibility of the donor and acceptor but will increase with phase separation [15]. As phase separation occurs and domain sizes increase, the efficiency of this step will decrease, reducing Jsc and PCE [15,32,33]. The domain crystallinities are also important since higher crystallinities allow for faster diffusion to the donor-acceptor interface [32].

Charge Transfer depends directly on electronic aggregation. Electronic aggregation will split the LUMO energy levels, which will change the LUMO-LUMO energy offset. Having an offset less than 0.2eV will cause a Jsc and PCE to drop [28]. Additionally, the HOMO level of squaraines can raise depending on its electronic aggregation [33,36,37]. This will cause a drop in the device Voc by reducing the energetic difference between the LUMO of the acceptor and the HOMO of the squaraine.

Lastly, charge dissociation depends on domain crystallinity and phase separation. The domain crystallinity can affect charge dissociation by increasing the charge carrier mobilities, which allows free charge carriers to move more quickly out of the effect of other free charge carriers, preventing recombination of charges [15]. Increases in recombination can manifest as decreasing Jsc, FF, and resulting loss of PCE [30]. Phase separation is important because the path length that the free charge carriers must travel is controlled by the domain size (and shape) and this is determined by the amount of phase separation [15].

Experimental Details

Now that we have established a firm background on how OPV and DOEs work we can discuss the specific DOE that was conducted and why it was set up the way that it was. If the reader will recall, we conducted a 6 factor, 2 level, full factorial DOE. The factors used were the blend ratio, the solvent additive, the concentration of the casting solution, the spin speed of the spin coater, and the annealing time and temperature. Table 1 shows the factors as well as the

high- and low-level values used. To complete the DOE, we needed to run 64 trials in random order. Appendix 1 details all of the trials.

Table 1: Table of factors and high- and low-level values.

Factor	High Level	Low Level
Concentration of Casting Solution	16mg/mL	12mg/mL
Blend Ratio	3:7	1:3
Spin Speed	2000rpm	1500rpm
Solvent	85/15 chloroform/DMA	85/15 chloroform/THF
Annealing Temperature	120°C	90°C
Annealing Time	15 min	5 min

There are three main assumptions made in our experimental design that must be acknowledged. The first assumption is that the trends in the response variables (PCE, Jsc, Voc, FF, and Failure Rate) are linear. We have made this assumption for two reasons. The first reason is that it allows us to do a two-level analysis and keep the number of trials required to determine significance to a minimum. This is especially important because we designed the largest possible type of DOE, full factorial. The second reason is that we are not particularly interested in finding optimal manufacturing conditions right now. We are interested in the overall significance of the interactions between parameters and how that can be used to gain greater understanding of the mechanisms that drive our devices. So, we only need to see the general trends and not the specifics. The second assumption we have made is that the amount of solvent additive used is negligible (i.e. we have not used it as a factor in the DOE), because doing so allows us to focus more on the significance of the type of solvent additive used (as will be explained below) rather than the details of optimization. We chose to use fix the amount of solvent additive at 15 % volume to be consistent with our previous work [38]. Lastly, we have held the amount of

solution deposited during spin coating constant at 66μL for comparison to our historical process and in an attempt to keep the size of the DOE manageable.

The question that remains is: why did we pick the factors and levels that we did? The short version is that all the factors chosen effect the microstructure of our devices and the levels chosen/selected have some basis in our historical process. As discussed above, the microstructure is critical to all the organic photovoltaic mechanics. The parameters we have chosen to effect the microstructure in different ways, detailed in Table 2, and our goal is to determine which ones cause a significant effect.

Before discussing the factors which we picked for this study, it is important to briefly cover the aspects of the microstructure which are potentially being affected and how they affect device process and properties. The active layer thickness is important to absorption because absorption is proportional to the path length that incident light must travel through an object. For solid objects, the path length is simply the thickness of the object. OPV devices are designed so that the only materials which absorb in the UV-VIS spectrum are in the active layer. Thus, UV-VIS spectroscopy measurements are dependent on the thickness of the active layer. Domain size is important to exciton diffusion and charge dissociation because the domain size dictates how far excitons and free charges, respectively, need to move before they return to the ground state [15,32,33]. The optimum domain size balances the need for excitons to easily reach the donor-acceptor interface, and the need for free charge carriers to move directly to an electrode [15].

The first factor selected for the study is the blend ratio. The blend ratio is the ratio of electron donor material to electron acceptor material. As can be seen from Table 2, it is important for two reasons. The first manner in which it is important is that it helps to dictate domain size. This is because, along with the concentration of the casting solution, the blend ratio contributes to the absolute amount of donor and acceptor materials and in a device's active layer. Additionally, the blend ratio can affect electronic aggregation and domain crystallinity. It has been shown with sqauraine:$PC_{61}BM$ films that as the weight percent of PCBM increases squaraine aggregation is reduced [15,32]. $DBSQ(OH)_2$:$PC_{61}BM$ films have been shown to be nanocrystalline upon casting, whereas neat $DBSQ(OH)_2$ films are mildly crystalline [15,39].

Table 2: Table of factors and what aspect of a device's microstructure they effect (along with the device process or property).

Active Layer Thickness (Absorption)	Domain Size (Exciton Diffusion and Charge Dissociation)	Aggregation (Charge Separation and Charge Carrier Mobility)
Concentration of the casting Solution	Annealing Time	Annealing Time
Spin Speed	Annealing Temperature	Annealing Temperature
	Concentration of the casting Solution	Solvent Additive
	Spin Speed	Blend Ratio
	Blend Ratio	
	Solvent Additive	

The levels of active layer we have chosen to test are 3:7 (30% electron donor to 70% electron acceptor) and 1:3 (25% electron donor to 75% electron acceptor). 3:7 is historically the ratio used in our process and so is a pertinent level for us to test. More importantly, we use this ratio because it is the ratio at which PCBM completely disrupts $DBSQ(OH)_2$ aggregation [15]. For the purposes of this DOE, 3:7 is the high level because it uses more squaraine. We chose 1:3 for our low level because we were interested to see if increasing the proportion of electron acceptor molecules provided any additional resistance to aggregation. We were especially curious, since many of the other factors (the solvent additive, the annealing time, and annealing temperature in particular) are likely to increase aggregation. We were also curious to see if this potential resistance to aggregation came at a cost to overall device efficiency.

The next factor we chose to investigate was solvent additive. The solvent additive can be thought of as a secondary solvent that is generally miscible with our primary solvent, chloroform. A solvent additive is used because the donor and acceptor materials have different

miscibilities/solubilities in the additive than they do in the primary solvent. The difference in solubilities will cause one material to start to crash out of solution first as the solvents evaporate (which will also happen at different rates). This can affect the domain size and aggregation within the domains by allowing more of one material to exist in the solid state than the other. Additionally, solvent, or solvent additive can become trapped within the material allowing a small amount of solvent annealing to occur until they evaporate. It has been demonstrated in devices made with 2,4-bis[4-(N,N-dipentylamino)- 2-hydroxyphenyl]squaraine that some combination of these effects can allow a squaraine to pack in a manner that increases device Jsc by 47.26% and improves PCE by 1.2% [38].

We chose our solvent additives to be tetrahydrofuran (THF) and dimethylacetamide (DMA).The difference between the solvent additive levels (DMA and THF) is of type and kind, rather than a quantitative difference in value. So, it was unimportant which we set as the high and low level. What is important about our solvent additives are the way in which they are different. DMA was chosen as a representative polar solvent additive and THF was chosen as a representative nonpolar solvent additive (both are organic solvent and have been used previously with squaraines by our lab) [38]. With this in mind we expected both additives to increase aggregation and affect Jsc and PCE as they have historically done [38].

The third factor which we have chosen to investigate is the concentration of the casting solution. Casting solution is the solution made with our solid materials, our solvent and our solvent additive that is spincast onto a glass substrate to form the active layer of a device. Because we have fixed the amount of solution that we actually spincast (66µl) the concentration of the casting solution dictates the amount of solids which are deposited. This will ultimately be important for determining the thickness of the active layer by potentially affecting the viscosity of the casting solution. We do not expect the concentration of the casting solution to affect the domain size or aggregation. This is because even though more material is deposited with a solution of increased concentration, the ratios of the donor and acceptor materials remain the same. In essence, we expect more domains due to increased active layer thickness, but of the same size and of the same aggregation that we would get at a lower concentration.

The levels we chose for the concentration of the casting solution were 16 mg/mL (the high level) and 12 mg/mL (the low level). 16 mg/mL represents a concentration slightly higher than what we typically use (15 mg/mL), while 12 mg/mL is significantly less. The purpose of

choosing these slightly extreme levels is to help to make obvious any effect on the device thickness and thus the absorbance of the active layer. Increases in the thickness of the active layer will increase absorbance. Increases in absorbance can lead to increases in Jsc [15,38]. However, increasing the device thickness also increases the average distance charge carriers need to move to reach an electrode, which can reduce Jsc. Given what we know about aggregation, we expect that factors such as the blend ratio and the annealing parameters will dominate the effects of the concentration of the casting solution and the spin speed.

We also chose to use spin speed as a factor. Spin speed is the rate at which our substrates rotate during spin casting. It is important not only to the thickness of our devices but also to the domain sizes in the active layer. As the spin speed increases, more material is thrown towards the edges of our substrates, making thinner active layers, and our solvents evaporate faster. This changing rate of solvent evaporation, especially when a solvent additive is used, can cause changes in domain sizes. Ultimately, the spin speeds used are bounded by the ability to make uniform thickness active layers which completely cover our substrates. Conducting a DOE uniquely positioned us to separate the effects of spin speed and our solvents, as well as looking at their combined effects.

The spin speeds we chose to investigate in this experiment were 2,000 revolutions per minute (RPM) and 1500 RPM. As stated before, these speeds were picked because they still produce uniform thickness films which completely cover our substrates. 1500 RPM is also the traditional speed used in our process. At lower rotation speeds, we start to struggle to completely cover our substrates, while speeds higher than 2000 RPM the film starts to “tear” and leave open spots on the substrate even if the substrate is covered to the edges. However, we don't expect the difference between our two chosen levels to be significant in and of itself, we are instead particularly interested in seeing if the spin speed interacts with solvent additive and casting solution concentration to produce thicker devices or larger domains.

The last factors we chose to look at in this experiment are the annealing time and temperature. It is easy to talk about these at the same time because they, ultimately, should have similar effects, since both parameters allow additional thermal energy to be added to the system. Given a fixed amount of time, higher temperatures will add more thermal energy to the system. Given a fixed temperature, a greater amount of time exposed to the thermal energy source allows more thermal energy into the system. In both cases, as more thermal energy is added to the

system, the microstructure of the active layer is driven further towards thermodynamic equilibrium. Since our devices are annealed immediately after spin coating, the annealing conditions can also affect how long residual solvent remains in the active layer. Residual solvent in the active layer allows small areas of the morphology of the active layer to continue to change after the initial casting. This can cause the formation of domains with greater aggregation than might be expected. If there is a general increase in aggregation it will be noticeable in absorbance. Increases in the size and quantity of crystalline domains should increase surface roughness, which is detectable with atomic force microscopy (AFM) [35]. Annealing a device that has residual solvent will cause the solvent to evaporate quickly but also increase the mobility of particles dissolved within the solvent until the solvent evaporates. The annealing time and temperature are expected to have large impacts on both the domain size and aggregation since squaraines and PCBM are not particularly miscible with one another. So, as the microstructure of the active layer approaches thermodynamic equilibrium, the materials phase separate, almost into a bilayer. Additionally, within large pure domains, squaraines tend to aggregate.

The levels for annealing time and temperature (high/low levels) are 15 minutes (min) /5 min and 120°C/90°C, respectively. A 15-minute anneal represents a very long anneal while a 5 minute anneal represents a short to mid-length anneal. Annealing at 120°C is a fairly high temperature anneal, while annealing at 90°C is more moderate. We chose both these parameters to investigate whether the path of approaching thermodynamic equilibrium is significant. The idea for doing so came from metallurgy where the rate of cooling and quenching is important to the microstructure [40]. We suspect that the combination of these two parameters will be more significant than either one individually. Additionally, coming from our understanding of polymer OPVs, we were interested to see if there was a sweet spot in the annealing time/temperature that would increase overall device efficiency.

At this point there are several main ideas that should be understood; the mechanisms and structure of OPV devices, the basic mathematical concepts behind DOEs, the key assumptions and experimental details, and the knowledge that the key mechanisms of OPVs are affected by the device microstructure and that all factors chosen for this DOE affect this microstructure. Our OPV devices are built in layers, starting with the glass, the transparent electrode, the hole transport layer, the active layer, and end with the metal backing electrode. The main mechanisms which allow them to work are absorption, exciton diffusion, charge separation, and charge

dissociation. The important assumptions that we have made are that we're only going to study one material pair ($DBSQ(OH)_2$ and $PC_{61}BM$), that we will deposit a fixed volume of casting solution, that we will be able to determine parameter significance from linear trends even if the trend is not truly linear, and that the amount of solvent additive we have chosen to use is enough to determine the significance of solvent additives but not so much as to skew the data to make solvent additives look more significant than they are. The factors in the levels chosen for use are displayed in Appendix 1. The aspect of the microstructure each factor affects, which is its reason for being chosen for this experiment, is displayed in Table 2 (which can be found near the top of the section).

Experimental Procedure

In this chapter, the procedures used for making devices and gathering data will be discussed. Additionally, the method of creating the data collection structure and order of experiments for a DOE will be discussed

DOE Structure and Order of Experiments

The order of experiments was created using MiniTab17. MiniTab is a software that is specialized for statistical analysis. Within MiniTab there is a DOE tool which simplifies the creation of the order of experiments. The number of factors (6), and the number of levels (2) were entered into the DOE tool. MiniTab then randomizes the order of experiments to avoid any bias in the results that may come from running similar trials back to back. The data recording structure was created by labeling the columns of the table produced by the DOE tool and adding columns for the PCE, Fill Factor, Jsc, Voc, and Failure Rate to be recorded.

Materials

There were several materials used to make the devices for this study, including soda-lime glass, aluminum, indium tin oxide, molybdenum (VI) oxide (MoO_3), $DBSQ(OH)_2$, and $PC_{61}BM$. The soda lime glass is used as the substrate for all our devices. The indium tin oxide (ITO) and aluminum serve as the positive and negative electrodes for devices. $DBSQ(OH)_2$ and $PC_{61}BM$ are solution processed to create the active layer. These materials were chosen, especially the chemical components, for their comparability to the recent literature from our lab [15,31,32,34,35,39].

The soda lime float glass was received from Visiontek Systems Limited, located in the United Kingdom, already coated with ITO. The ITO is then etched in-house to create the pattern necessary for our devices. MoO_3 starts as a powder received from Sigma Aldrich (>99.5% purity) and is evaporated onto the substrate to act as a hole transport layer. Aluminum starts off as aluminum shot made by Alfa Aesar (>99.999% pure) and is evaporated onto a device in the last step of manufacturing. The $DBSQ(OH)_2$ is manufactured at RIT by Dr. Jeremy Cody's research group [15,31]. Lastly, PC61BM was sourced from several suppliers with each new bottle being verified as acceptable when opened (see below). The purity of all $PC_{61}BM$ was

99.5%. Additionally, chloroform, dimethylacetamide (DMA), and tetrahydrofuran (THF) were used as solvents during solution processing and spin coating. These chemicals were all received from Sigma Aldrich.

PCBM Acceptance

Because the PCBM used for this study was sourced from multiple manufacturers it was necessary to develop an acceptance test for bottles received from a new manufacturer, to verify consistent absorbance behavior. The test consisted of making a UV-VIS spectroscopy sample from the new material and comparing it to the UV-VIS spectrum of a sample made from the first bottle used. The spectra were compared to verify the general shape of the spectra and the peak locations. However, this only confirms the optical properties of the PCBM and serves as a very low-level purity confirmation. Electronic devices and testing are generally more sensitive to impurities then this test. Each sample was a neat film of $PC_{61}BM$, produced by taking 7 mg of $PC_{61}BM$ and diluting it to a concentration of 16 milligrams per milliliter in 437.5 μL of chloroform. A microscope slide, cut to be roughly 25mm square and cleaned with successive acetone and IPA baths in a sonicator, was then spin coated with 66 μL of the solution. A Shimadzu UV-2600/2700 series spectrophotometer was used for this test, and all others.

Device Manufacture

Making devices is a relatively long process that generally takes two and a half to three days of work by one or two students in the lab. Because the process is so lengthy, it is easier to think of it in terms of several subprocesses. These subprocesses are, in order: ITO etching, substrate cleaning, MoO_3 deposition, solution preparation and spin coating, annealing, and aluminum deposition.

ITO Etching

By etching the ITO covered glass that the lab receives from Visiontek so that the ITO creates a pattern, we are able to make and test 8 devices on each substrate. This is helpful for ensuring repeatability and reducing the number of substrates we need to use. To do this we utilize the cleanroom present in the Semiconductor and Microsystems Fabrication Laboratory

(SMFL) present at RIT. The ITO glass is first cleaned with acetone, IPA, and deionized water and air dried. After air drying, HPR-504 photoresist is spin coated on each glass plate at 2000 rpm. Then the plates are soft baked at 120°C. A chromium mask designed by Chenyu Zheng is placed on the same surface as the photoresist. The plate and mask are then exposed to mercury broadband irradiation to degrade the exposed photoresist. Then the mask is removed, and the photoresist is developed with CD-26 positive developer removing any photoresist which was exposed to radiation. Then the plate is hard baked at 120°C. Lastly, the plate is etched to remove any ITO that no longer has photoresist on it using a one-to-one solution of hydrochloric acid and deionized water. This process is conducted with the glass plates on a hot plate set to 100°C while the etchant is between 35°C and 55°C. The actual etching takes 10 minutes. The now etched plates are rinsed with acetone, isopropyl alcohol (IPA) and deionized water to remove any unexposed photoresist. For this study, these steps were primarily performed by Zhila Hooshangi and Tyler Wiegand. Lastly, the etched plates are shipped to West Scientific Glass in Webster, New York to be cut to the final substrate size of 20mm by 15mm.

Substrate Cleaning

After the substrates return from West Scientific Glass, they are cleaned using the following process. First, substrates are placed in an acetone bath, in a sonicator for 15 minutes. This is repeated using IPA. They are then rinsed in boiling deionized water and dried with forced air. After air drying, the substrates are then baked until there is no water visible on any surface of the substrate. The last step in cleaning is to expose the substrates to Ozone for 20 minutes to remove any organic residue that may be on the surfaces of the substrate.

MoO_3 Deposition

MoO_3 deposition is accomplished using a COVAP II 200/400 evaporator made by Angstrom Engineering. The evaporator and the mask used in this step are within a nitrogen glove box. Up to 12 substrates at a time are placed in a shadow mask that was designed by Chenyu Zheng. The substrates are placed in the mask so that the ITO on the substrate is exposed. Deposition will result in a 12nm thick layer of MoO_3. The mask is placed in the evaporator, and then the amount of MoO_3 powder in the tungsten evaporation boat is checked by inspecting how

dark it is. If the color is too dark more powder is added. Every 5 cycles the boat is changed and new powder is used with it. If these levels are appropriate, the evaporator is then sealed, and the pressure brought down to less than 2.00×10^{-6} Torr. This generally takes between 3 and 6 hours. Once the vacuum pressure is reached the deposition profile designed by Chenyu Zheng is run. Once this step is complete the substrates are ready for spin coating.

Solution Preparation and Spin Coating

Generally, while waiting for the evaporator to reach appropriate vacuum pressure, the active layer solutions are prepared. The appropriate amount of each chemical, DBSQ(OH)2 and $PC_{61}BM$, are weighed out in a vial, recording the actual amounts used. The total mass is then entered into a solvent calculator spreadsheet to determine the correct amount of solvent and solvent additive to use, so that the solution is always diluted to the correct concentration and that the ratio of solvent to solvent additive is always correct for the trial being run. Then the solvent and solvent additive are added to the vial with the actual amount used recorded. The vials of solution are then placed in the sonicator for 10 minutes to ensure that all the solute is completely dissolved. After sonication, solutions were immediately transferred to a nitrogen-filled glove box and were stored there until spin coating. Solutions were never stored for more than 6 hours before spin coating.

After solutions are prepared and MoO_3 deposition is complete, substrates were spin coated, using an Ossila 2.0 spin coater. This process is also done in a nitrogen glove box. Substrates are placed with the ITO side up in the jig in the spin coater. 66µL of solution is deposited on the substrate and spun for 30 seconds at a spin speed determined by the order of experiments. Note that it is important that the spin coater is started as soon as the solution is deposited on the substrate. This is because the volatile solvent begins to evaporate almost immediately, and the rotation of the spin coater is essential for an even coating. Once all the substrates have been coated, they are ready for annealing. The remaining active layer solutions are used to make spectroscopy samples for additional analysis. Annealing should be carried out immediately after spin coating, though it is ok to spin coat all the devices being worked on and then anneal them all as necessary, with this time difference being insignificant.

Annealing

Immediately following spin coating all the substrates are annealed using a hot plate. Annealing parameters (time and temperature) are determined by the trial "recipe". The hot plate used for annealing is stored within the nitrogen glove box. For consistency, all devices in this study were annealed with the ITO/active layer side up with the bare glass side on the hot plate. Temperature of the hot plate was verified by a laser thermometer (Laser Grip 1080) measurement at approximately the center of the hot plate. Devices were then placed as close to the center as possible. Immediately after annealing all devices were moved into the evaporator for aluminum deposition.

Aluminum Deposition

Aluminum deposition also uses an evaporator in a nitrogen glove box. It also uses a shadow mask, though a different mask from MoO_3 deposition. Substrates are placed in this mask so that the active layer side is exposed, and then placed in the evaporator. Two pieces of aluminum shot, with diameters between 2mm and 4mm, are placed in the evaporator in a tungsten evaporation boat. The boat is replaced every 5 cycles. Then, like in MoO_3 deposition, the evaporator must come down to a pressure of 2.0×10^{-6} Torr before the deposition program designed by Chenyu Zheng can be run. After the evaporator is run, devices can be held under vacuum for up to 24 hours before testing, though it is best practice to test them immediately to ensure that the active layer does not degrade.

Spectroscopy Samples

Spectroscopy samples are made in much the same way as the $PC_{61}BM$ acceptance samples described above. The major difference being that instead of creating a neat film, the film created has the same makeup as the active layer of a device. Typically, these samples were made from the exact same solutions that devices were made from but on a for trials 1-6 the solution had to be remade because spectroscopy samples were made significantly later than the corresponding devices. Note that once a spectroscopy sample is made it is considered stable for much longer than a device because spectroscopy is less sensitive to defects then electronic testing, and so spectroscopy data was collected up to a week after the slide is made.

Performance Testing

To test the performance of our devices they are exposed to light from a Newport 91192 solar simulator at a power of 100 mW/cm^2. The solar simulator is calibrated monthly for accuracy. Device performance measurements were taken using a Keithley 2400 Sourcemeter using a 4-point probe. The procedure for testing is to first place the device, glass side down, on the viewport above the solar simulator. Then, the probes are placed, with one on the aluminum electrode and one over the ITO. A -2V to 2V sweep is initiated using LabView software which controls the sourcemeter and records current values. Simultaneously, the aperture of the solar simulator is opened, exposing the device to light from a 450-watt Xenon arc lamp. Once data is recorded, it is copied into an Excel spreadsheet which is designed to generate not only the J-V curve from the sweep but also to calculate PCE, FF, Jsc, and Voc. Data is recorded in text file and copy/pasted into the spread sheet, allowing the J-V curve to be plotted as well as current (J) and power (P) to be calculated for every point. J is the recorded I divided by the surface area (SA) of a device (and multiplying by 1000 to get J in mA/cm^2). Jsc is determined by finding the J when voltage, V, is zero. Voc is found by detecting when the sign of J switches and linearly interpolating for the value of V when J would be zero. FF is found by first determining the maximum power and then dividing by Voc times Jsc and SA, $F = \frac{P_{max}}{Voc*Jsc*SA}$. PCE is calculated similarly, by dividing P_{max} by the incident solar power ($P_{incident}$), SA and a factor of 0.0001 to correct units, $PCE = \frac{P_{max}}{P_{incident}*SA*0.001}$ .The data acquisition system and the Excel spreadsheet were created by Chenyu Zheng. In order for accurate data to be taken, the probes must register a stable current before the voltage sweep is initiated. At the time of this study, experience was the best judge to determine if the current is stable enough, as it can vary from device to device and from batch to batch. We have since found, courtesy of Tyler Wiegand, that excess active layer (that which is on the substrate after casting but not part of a device) can be removed with a cotton swab dipped in chloroform to expose the ITO layer. This allows the probs to make good electrical contact with the ITO and Aluminum electrodes producing much more stable readings. Any device that does not stabilize is counted as failed when calculating failure rate. Additionally, any device whose current-voltage curve did not match the curve that a diode would produce was also counted as failed.

UV-Vis Spectroscopy

The spectrophotometer used for this data collection is a Shimadzu UV-2600/2700 series spectrophotometer. The device settings used were a scan from 300 to 900 nm wavelengths at increments of 1 nm with a slit width of 2 nm. Baselines were taken before each round of testing, using a similar, uncoated, clean piece of microscope glass. Spectroscopy data was used during analysis to help explain trends in the DOE.

SEM Imagining

SEM imaging was done using a Hitachi S-4000 SEM on spectroscopy samples. Copper tape was used to electrically connect the active layer to the grounded sample holder. SEM imaging was also used during analysis to help explain trends in the DOE.

Metrics

This section will go through an explanation of the measurements taken. We tested for power conversion efficiency (PCE), fill factor (FF), short circuit current density (Jsc), open circuit voltage (Voc) and failure rate. Before presenting data, each of these metrics will be explained along with why we use it, how it was calculated. The presentation of the data will highlight some impressively high and impressively low values as well as some of the basic trends.

Power conversion efficiency, or PCE, is a measure of how well devices convert solar radiation energy to electrical energy[31]. PCE is the main metric used to compare devices to each other, with higher efficiencies indicating better devices[31]. .PCE is the product of the efficiencies of the individual steps in the charge photo-generation process, discussed above, meaning PCE is also the ratio of the device power output to the power of the solar radiation which hits the device.[31,41] However, PCE cannot be directly measured, it is determined using the measured values of Jsc, Voc, and FF. These values are multiplied together and then divided by the power density of the radiation source, as shown in Equation 2, to determine PCE.

$$PCE = \frac{V_{oc} J_{sc} FF}{P_{incident}} \tag{2}$$

Fill Factor, or FF, is a measure of how ideally a device performs [15]. Specifically, FF is the ratio of the maximum measured device power to the ideal maximum power based on the Jsc and Voc values. This ratio is called “fill factor” because power is the integral of IV (in our case we are really looking at power density, which is the integral of JV) or the area of a rectangle. This ratio describes how the real integral “fills” the rectangle of the ideal integral, thus the name fill factor, as shown in Figure 7. The fill factor is important because it, in combination with Jsc and Voc, allow us to determine if changes in PCE are due to changes in electrical properties (seen as changes in Jsc or Voc) or due to changes in the efficiencies of the photon to electron conversion process (seen as changes in FF or Jsc).

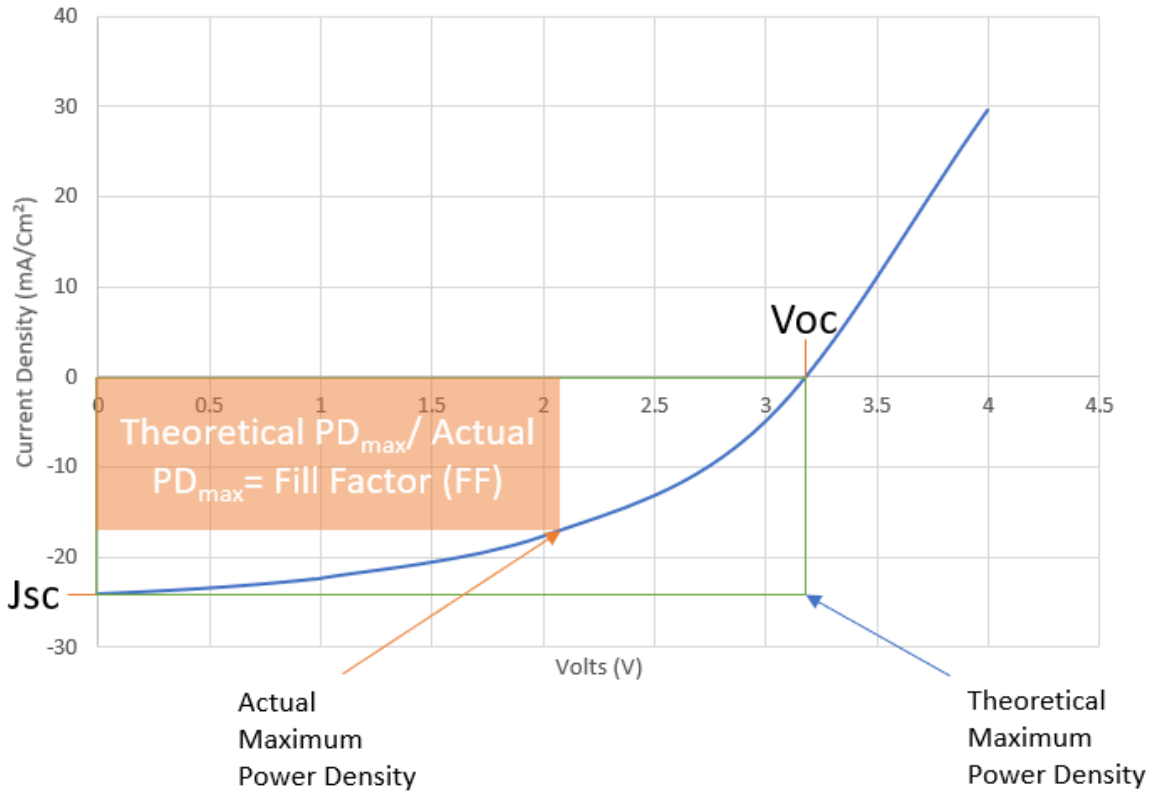

Figure 7: Graph of a hypothetical JV curve produced by a hypothetical OPV device (not to scale with what our devices produced) while illuminated The Voc and Jsc are labeled and an attempt is made to depict the FF(the ratio of the actual maximum power to theoretical max power).

The short circuit current density, or Jsc, is the current density when the device is electrically shorted. In other words, Jsc is the current density when there is no voltage across the device. Current density, J, can be measured directly by our equipment and Jsc can also be determined by the y-intercept of a JV curve. Jsc, along with Voc is important to understanding how theoretically optimized our devices are because these values determine the theoretical maximum efficiency.

The open circuit voltage, or Voc, is the voltage across the device when the circuit is open, or when there is no current through the device. Much like J and Jsc, V can be measured directly by our equipment and Voc is determined from the JV curve as the x-intercept. Again, the Voc and Jsc are important because they define the theoretical maximum efficiency of a device.

Failure rate is the percentage of devices in a trial that do not work. It is calculated by taking the number of devices that do not work (as described earlier) and dividing by the total number of devices in each trial (32 total). It is used primarily to critique how well a given trial

makes devices. We are interested to see if there is a correlation with decreased failure rate and increased device efficiency.

DOE Results

Below, in Table 3, is the data recorded for the DOE along with the trial "recipes" which produced the data. There are several things to note in the data. First, there are only twenty-one completed trials. This was due to various technical difficulties and supply issues that arose during the process of conducting our experiment and will be the subject of Analysis Two of this study. Additionally, certain cells are highlighted in the data. The bright green highlighted PCE value is the highest value, 2.5%. This is within the typical range of efficiencies for $DBSQ(OH)_2$. The faded green FF values are > 45%, which represents an elevated FF from what is typically seen. The faded green Jsc values are <-7 mA while the faded red values are >-1mA (noting that more negative current is desired). The faded green Voc values are >0.7V and the faded red values are <0.1V. The bright red failure rate values are > 66.67%. Two thirds of a trial's devices failing was taken to be problematically high for industrialization.

Table 3: Table of factors, the trials that were run and their results. The bright green highlighted PCE value is the highest value, 2.5%. This is within the typical range of efficiencies for DBSQ(OH)2. The faded green FF values are > 45%, which represents an elevated FF from what is typically seen. The faded green Jsc values are <-7 mA while the faded red values are >-1mA (as more negative current is desired). The faded green Voc values are >0.7V and the faded red values are >0.1V. The bright red failure rate values are > 66.67%.

Concentration of Casting Solution (mg/mL)	Blend Ratio (mg:mg)	Spin Speed (rpm)	Solvent Additive	Annealing Temp. (°C)	Annealing Time (mins)	PCE (%)	FF (%)	Jsc (mA)	Voc (V)	Failure Rate
16	3:7	2000	THF	120	5	2.05	44.33	-6.669	0.683	68.75%
16	3:7	2000	THF	90	15	2.50	41.58	-7.594	0.787	31.25%
16	1:3	1500	THF	120	5	2.11	46.09	-6.186	0.739	28.13%
16	1:3	1500	DMA	90	15	0.00	0.00	0.000	0.000	100.00%
16	3:7	1500	DMA	90	5	0.00	0.00	0.000	0.000	100.00%
16	1:3	1500	DMA	120	5	0.00	0.00	0.000	0.000	100.00%
16	3:7	1500	DMA	120	15	0.00	0.00	0.000	0.000	100.00%
12	1:3	1500	THF	120	5	0.73	21.60	-4.653	1.843	93.75%
16	1:3	1500	THF	90	5	1.47	36.28	-4.631	0.936	68.75%
16	3:7	1500	DMA	120	5	0.00	0.00	0.000	0.000	100.00%
12	1:3	1500	DMA	90	5	0.00	0.00	0.000	0.000	100.00%
12	1:3	2000	DMA	90	15	0.00	0.00	0.000	0.000	100.00%
12	3:7	1500	DMA	90	5	0.00	0.00	0.000	0.000	100.00%
16	1:3	2000	DMA	90	15	0.00	0.00	0.000	0.000	100.00%
12	3:7	2000	THF	120	5	1.79	49.14	-4.685	0.782	87.50%
12	3:7	1500	DMA	120	15	0.00	0.00	-0.702	0.002	100.00%
12	3:7	2000	DMA	90	5	0.00	0.00	-0.789	0.002	100.00%
12	3:7	2000	THF	90	5	2.36	51.40	-5.800	0.791	50.00%
16	1:3	2000	DMA	120	15	0.00	0.00	-0.621	0.002	100.00%
16	1:3	2000	THF	90	15	2.20	50.10	-5.587	0.788	6.25%
16	3:7	2000	DMA	90	5	0.00	0.00	-0.897	0.002	100.00%

Analysis

Despite the fact the entirety of the DOE could not be completed there are still interesting conclusions which can be drawn from the data that was collected/from the trials that were completed. The first is that the solvent additive is hugely significant to device performance and process performance. This is evidenced by the failure of all devices made with DMA as the solvent additive. There was a 100% failure rate of these devices in the data recorded. The solvent additive is significant to the aggregation of material in the active layer because the materials used in the active layer will have different solubilities in the additive than in the main solvent and the solvent and additive have different evaporation rates [38]. With this in mind, we went looking for evidence of phase separation and aggregation. To do this we use two techniques. First, we used a scanning electron microscope to look for phase separation. Then we used UV-VIS spectroscopy to confirm aggregation. The SEM allows for the visual scanning of a substrate for surface features which may show phase separation of materials. UV-Vis spectroscopy will allows to determine if what we see in the SEM is aggregated because aggregation is linked to specific peaks in the absorbance spectra of squaraines [15,31,34,36,38].

Below in Figure 8 are SEM images of the active layers made in two different ways. The first image (left) was taken of an active layer made with THF as the solvent additive. The second image (right) was taken of an active layer made using DMA as the solvent additive. Both images were taken on the same SEM at 1000 times magnification. The difference is striking, at this magnification the THF active layer appears fairly uniform and mostly gray with some small white flecks. The DMA active layer, however, appears to have stark white ridges as well as white splotches in the film. The darkening of approximately two-thirds of the image is most likely due to electron burn from the SEM. This data was taken using only the two slides mentioned. However, the THF slide chosen was several months old, and was deliberately selected to present a worst case example of that microstructure (knowing that materials can anneal over time to approach the thermodynamic equilibrium and possibly towards phase

separation), while the DMA slide was no more than two weeks old to try and look at a best case example of that microstructure.

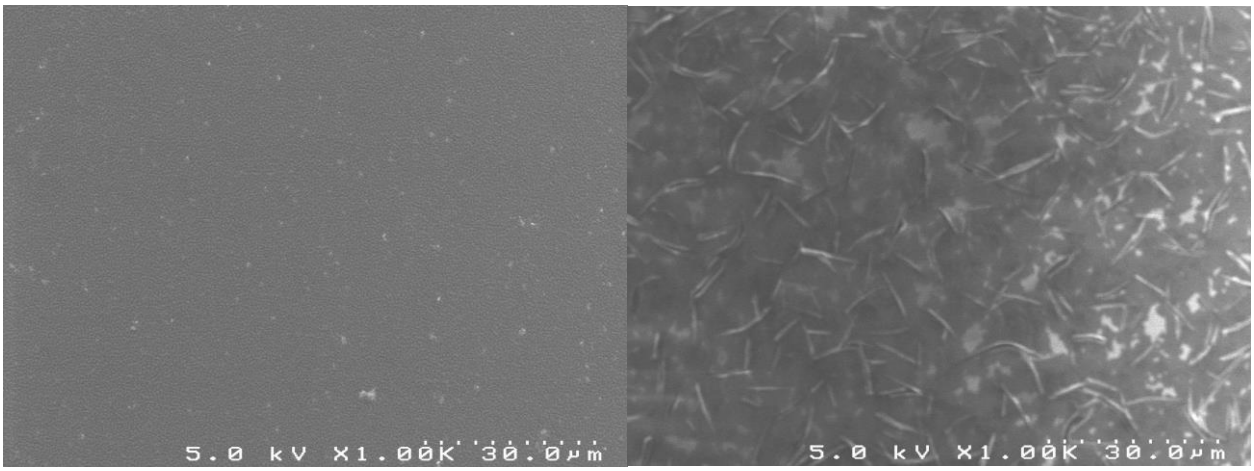

Figure 8: SEM images active layers as they appear on spectroscopy slides. THF was used as the solvent additive (left). DMA was used as the solvent additive (right).

To determine whether the phase separation and crystallization seen in devices made with DMA was also aggregated we looked at the UV-VIS absorption spectrum of our devices. Due to the apparent crystallization seen in the SEM images, we expected the spectra of our devices to show an increased peak associated with the H-aggregate. Any double hump spectrum observed within the range where DBSQ(OH)2 absorbs indicates some aggregation, but from the SEM images we expect a larger H-aggregate peak than monomer peak. However, this is not what we found. It appears that the devices made from DMA, generally, suffered lower absorbance than those made with THF, as shown in Figure 9, which shows the composite minimum and maximum absorbances of devices made with DMA to be shifted down from the those of the devices made with THF. This is interesting because it shows devices made with DMA are not absorbing as much light as those made with THF. This is important because absorbance is the first step in the photon to electron conversion presses, if it is significantly limited, the PCE of a device will suffer. Ultimately, the lack of agreement between what we thought we were seeing in the SEM images and the absorbance spectra, we speculate that the DMA devices are failing either because excitons are recombining before charge transfer can occur or the path to the electrodes for separated charges are too long. We have not gathered the information to tell

which. Additional experimentation that could help solve this would include fluorescence quenching experiments to determine if charge transfer is occurring.

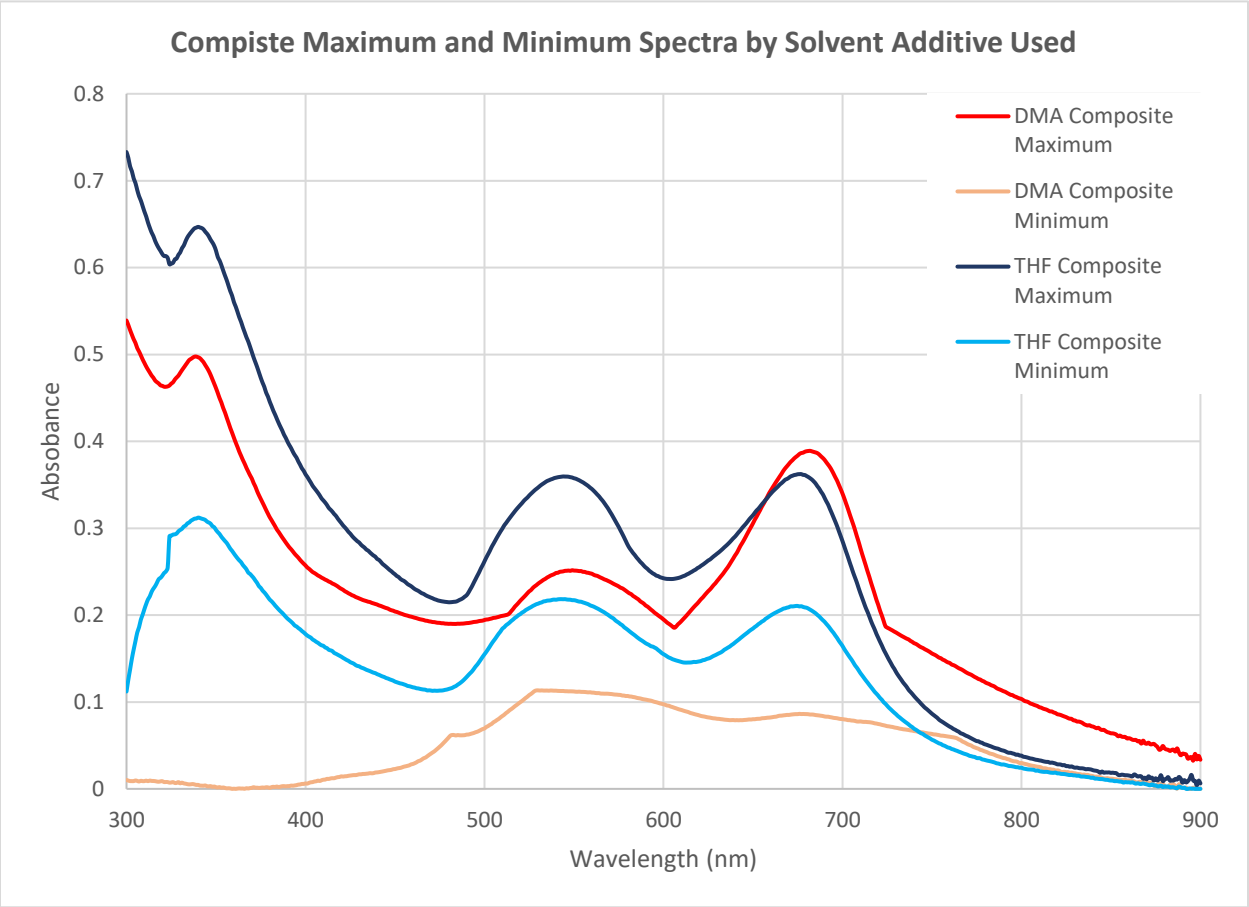

Figure 9: Graph of the composite minimum and maximum spectra by the solvent additive used. "Composite" indicates that each data point is the maximum or minimum (depending on which spectrum is looked at) absorbance for a given wavelength of all devices made with the indicated solvent additive.

Based on the literature[15,33–35] we expected that annealing devices at 120°C would produce devices with lower PCE than devices annealed at 90°C, because hotter temperatures allow squaraine to aggregate faster . We also expected that devices annealed for 15 minutes would produce lower PCEs than devices annealed for 5 minutes because annealing for longer periods of time allows more time for squaraine aggregation. Additionally, we expected all of the annealing conditions to produce devices that were less efficient than the average unannealed device of the same blend ratio [15,33–35]. The reason being that spin cast films of $DBSQ(OH)_2$:PCBM blends tend to be well mixed when cast, and so annealing, even mildly, causes significant enough squaraine aggregation to reduce PCE [15]. Table 4 shows the weighted average PCE value of all trials where THF was used as the solvent additive, grouped by

annealing conditions. Devices where DMA was used as the solvent additive will be ignored from here on out since they were not counted as working devices.

Table 4: Table of average PCE values of devices produced at different annealing condition and the weighted standard deviation of the average PCE across multiple trials with the same annealing conditions.

Weighted Average PCE by Annealing Condition					
	Annealing Temperature				
Annealing Time		120°C	Standard Dev.	90°	Standard Dev.
	15 minutes	no data	no data	2.33%	0.20%
	5 minutes	1.99%	0.36%	2.02%	0.49%

Looking at Table 4, we see that the expected trend in temperature appears true, since both 90°C annealing conditions (5 minutes, and 15 minutes) have higher weighted average PCEs than the weighted average PCE of devices annealed at 120°C for 5 minutes (which we expect to be the more efficient of the two 120°C annealing conditions). Looking at Table 5, where weighted average PCE is determined by blend ratio, we can see that neither historical average PCE is exceeded. Looking back at Table 3, no individual trial average efficiency exceeds the historical average PCE for the respective blend ratio.

Table 5: Table of average PCE values of devices produced using different blend ratios and the weighted standard deviation of the average PCE across multiple trials with the same blend ratio.

Average PCE by Blend Ration				
Blend Ratio (mg:mg)	Experimental Average PCE (%)	Standard deviation (%)	Historical Average PCE [15]	Standard deviation (%)
3:7	2.33%	0.26%	3.02%	0.08%
1:3	2.01%	0.39%	2.52%	0.08%

Our expectation that 5 minute anneals would produce more efficient devices than 15 minute anneals was not met. This can be seen in Table 4, where the highest weighted average PCE belongs to the devices that were annealed at 90°C for 15 minutes and not to the devices

annealed at 90°C for 5 minutes. Table 6 displays the device performance metrics, Jsc, Voc, and FF as weighted average values grouped by annealing conditions. In Table 6 we see that the primary differences between the two 90°C anneals is that the 15 minute anneal has an increased Jsc (more negative) and decreased Voc when compared to the 5 minute anneal. In the literature, the drop in Voc is attributed to the splitting of molecular orbitals/energy levels that occurs because of aggregation [31,33,36,37]. The splitting of the energy levels effectively raises the HOMO energy level of the squaraine, reducing the difference between the HOMO of the squaraine and the LUMO of the $PC_{61}BM$, thus reducing Voc [31,33,36,37]. The overall rise in PCE from the 90°C/5 minute anneal to the 90°C/15 minute anneal happens because the rise in Jsc outweighed the drop in Voc. The rise in Jsc is most likely due to an increase in the EQE of the H-aggregate as was seen in a similar case (where a Jsc rise outweighed a Voc drop, causing an annealed device to outperform expectations) documented by Chenyu Zheng [31]. However, here we have not performed EQE measurements; doing so would help to confirm the cause of the Jsc rise.

Table 6: Table of device performance parameters (as weighted averages) and their associated weighted standard deviation.

Weighted Average Jsc, Voc, and FF by Annealing Condition						
Annealing Condition	Jsc (mA/cm^2)	Standard deviation (mA/cm^2)	Voc (V)	Standard deviation (V)	FF (%)	Standard deviation (%)
90°C for 5 min	-5.350	0.657	0.847	0.081	45.58%	8.49%
90°C for 15 min	-6.436	1.145	0.788	0.001	46.50%	4.86%
120°C for 5 min	-6.077	0.730	0.786	0.286	44.70%	6.38%

Conclusion

Recall, the ultimate goal of this work was to determine the assembly paradigms of $DBSQ(OH)_2$:$PC_{61}BM$ films and to model how they are affected by manufacturing parameters to work towards the construction of a more general model for optimizing OPV devices based on the donor and acceptor selected. In order to achieve this goal, we continue to advocate for the use of DOEs to study OPVs because they provide a rigorous and robust methodology while screening variables and interactions for which ones will drive predictive models of device performance.

The experimental rigor, its thoroughness, of DOEs comes from many of its well documented features. These features include the investigation of multiple parameters at once, determining the significance of interactions between parameters, and allowing for efficient experimentation. A full discussion can be found above in the sections *What is a Design of Experiments (DOE)* and *Review of How DOEs Add Value to the Analysis of Complex Systems* but will be summarized here. Investigating multiple variables at once and determining the significance of interactions between variables provides DOEs with increased experimental rigor by comparison to OVAT analyses. By investigating multiple parameters at a time DOEs can condense the work of many studies into one. Determining the presence of and significance of interactions between variables can only be done by examining multiple variables at once and allows DOEs to help design processes by more completely understanding how process steps will affect one another. Being able to gather this increased information in the same number of, or often fewer, trials increases the rigor still further and makes DOEs very efficient studies. These elements of increased experimental rigor allow DOEs to more efficiently develop more complete models of the system that they are used to study [10–12].

The robustness of DOEs, their ability to handle many situations, can be shown by the many kinds of systems that they can be used with, including OPV. DOEs were invented in the 1920s by Sir Ronald Fisher to study the effects of fertilizers [10]. Yet, Antony opens his text examining a chemical process where temperature and pressure can be varied, and demonstrates how a DOE would have been the better tool for analyzing the system [10]. We have demonstrated above (in *Review of How DOEs Add Value to the Analysis of Complex Systems*) how two studies from the OPV literature could have been improved as DOEs. Both studies, one by Zhu et. Al and one by Zheng, could have been done in less trials and Zheng's study could

have expanded its scope to completely examine all the electron donors used with both electron acceptors used [14,15]. Despite the different fields these example systems belong to, DOEs are robust enough to study them all.

Despite its incompleteness, the DOE which we have conducted makes clear the overwhelming significance of the use of solvent additives to device performance and production yield. We saw all the devices made using DMA (chosen to be a representative polar solvent additive) fail. Our data indicates that this is due to massive phase separation between the $DBSQ(OH)_2$ and $PC_{61}BM$ domains. This simple conclusion is not without great value, because it presents the possibility of two paradigms. In the first, solvent additive effects can be dialed in to improve device performance, we suspect by controlling the polarity of the solvent mixture (the mixture of solvent additive and main solvent). If this is the case, the optimization of squaraine based OPVs could be reduced to the tuning of the polarity of the solution mixture. In the second paradigm, the effect of solvent additives cannot be controlled and so the use of solvent additives must be eliminated from production of squaraine based devices.

The suggestion of these two paradigms allows us to examine how variables may be screened using a DOE (though normally this would happen after the completion of a DOE when determining the path forward). Once it is determined that a parameter is significant it can be spun off into other analyses to model its effects more precisely. This is what is required to investigate the first paradigm from above and could be done by conducting an OVAT analysis of solvent mixture polarity vs. device performance and manufacturing yield. We find an OVAT appropriate for this analysis because we are confident that the output response will only depend on one variable and wish to determine how the response changes with this variable in high detail. If it were determined that the solvent mixture polarity could not be used to dial in solvent additive effects to improve devices, we would then operate under the second paradigm. In this paradigm the solvent additive is screened out of future analyses allowing for a reduced DOE of 5 factors (2 levels, full factorial) in 32 trials to be conducted. It is worth noting that this kind of in-process screening of parameters is not advised as it circumvents the rigor of a DOE. Screening of parameters should take place after the completion of a DOE to ensure that the correct parameters are screened and is only suggested as something that we could have done during experimentation because of the strength of the effect of DMA, supplemental data SEM, and spectroscopy data (Figures 8 and 9) that corroborated the incomplete DOE data.

Our recommendation for the continued use of DOEs to study OPV does not come without understanding its draw backs. The main tradeoff of conducting a DOE is that in exchange for increased experimental rigor, there must also be increased rigor in setting up and planning. Failing to set up and plan correctly will lead to a DOE being resource draining, difficult and time consuming to complete. Additionally, the heightened experimental rigor cannot yield its value without consistent and true data making it critical to ensure the reproducibility of the process being studied and accuracy of measurement of data. The reproducibility of the process being studied may be affected by both equipment reliability and the measured precision for a particular process step or set of steps. In our case, our process relies heavily on the functionality of our spin coater. When it starts to fail, so do our devices due to uneven or incomplete coating of the active layer. In order to avoid losing valuable time, it is important to know how to detect when critical equipment begins to fail, and to have spare components or spare equipment on hand. In the case of our spin coater, we know they are operable for a few years and have a standard device trial to determine the condition of the spin coater.

Our process also relies on measuring out $DBSQ(OH)_2$ and $PC_{61}BM$ by hand. This can make it very difficult to repeat a blend ratio exactly, as well as being time consuming, and tedious. The precision of the balance used, also leaves something to be desired, with a precision of only 0.1mg. Improving the precision of the balance will help with knowing how well the blends are reproduced and help slightly with the accuracy, by allowing the operator a better understanding of when they are approaching the correct amounts. However, more significant gains could be made by changing the way in which the materials are measured out. One option would be to use whole bottles of stock materials at a time, since they are accurately weighed out by the manufacturer, to create stock solutions. Given the concentration of a solution, it is very easy to determine how much to use to capture an amount of solute. This can be done with great accuracy using pipettes. Similarly, a researcher could approximately weigh out several batches at a time, unmixed, and then calculate the amount of solvent required to obtain a standard concentration. Challenges to both these approaches arise from the solvent used. Given the highly volatile nature of chloroform, it is very important to properly store a solution made with it, as solvent evaporation will change the concentration. Some other ideas include using an Archimedes screw [42], or shaker table to dispense material at an even and controllable rate. The Archimedes screw would be particularly accurate as its action can be stopped at any time with

greater precision, though it does require a minimum amount of material to operate properly [42]. OPV is, of course, not the only field where the weighing of light powders is an issue, and additional solutions may be found across disciplines; pharmacy comes to mind as an industry where powders are frequently measured out in similar amounts to what we have used here [42] and may have more solutions to help ensure the reproducibility of DOEs conducted on OPV systems.

Lastly, there is the need to ensure the accuracy of measurements when taking data. It is our experience that difficulties here can come from poor understanding of how the testing set up interacts with a device. In the four-point probe set up used here, the probes were required to pierce the active layer to contact the ITO electrode underneath. This can cause poor electrical contact between the probes and the ITO electrode. In turn, this can lead to an unstable current reading. Recall from the experimental procedure that data could only be taken from devices with a stable current, that devices that were unstable were counted as failed, and that until this issue was addressed, experience was the best way to tell them apart. This was addressed by Tyler Wiegand and now we remove excess active layer before testing to expose the ITO electrode, allowing the probes to make good electrical contact, and ensuring accurate and reproducible data. To approximate the significance of this change, two batches of the standard set of devices mentioned above (usually used to check on the health of the spin coater) could be made. Where one batch is tested without removing excess active layer, and the other after removing excess active layer and determining the difference in the failure rates.

Despite increased requirement for rigor when setting up and planning a DOE, our recommendation for the use of DOEs to study OPVs remains strong because we have found that the increased rigor, and overcoming the associated difficulties, adds robustness to our manufacturing and data collection processes. By forcing the development of robust processes DOEs not only provide a rigorous and robust methodology for the study of OPVs while also screening variables and interactions for which ones will drive predictive models of device performance, but also move us toward processes that are robust enough to be scaled up when it is becomes time to bring OPVs to market.

Appendix I: Table of Individual Trial Specifications

Trial number	Concentration of Active Layer	Blend Ratio	Spin coat Speed	Solvent Additive	Annealing Temp.	Annealing Time
1	16	3:7	2000	THF	120	5
2	16	3:7	2000	THF	90	15
3	16	1:3	1500	THF	120	5
4	16	1:3	1500	DMA	90	15
5	16	3:7	1500	DMA	90	5
6	16	1:3	1500	DMA	120	5
7	16	3:7	1500	DMA	120	15
8	12	1:3	1500	THF	120	5
9	16	1:3	1500	THF	90	5
10	16	3:7	1500	DMA	120	5
11	12	1:3	1500	DMA	90	5
12	12	1:3	2000	DMA	90	15
13	12	3:7	1500	DMA	90	5
14	16	1:3	2000	DMA	90	15
15	12	3:7	2000	THF	120	5
16	12	3:7	1500	DMA	120	15
17	12	3:7	2000	DMA	90	5
18	12	3:7	2000	THF	90	5
19	16	1:3	2000	DMA	120	15
20	16	1:3	2000	THF	90	15
21	16	3:7	2000	DMA	90	5
22	12	1:3	1500	THF	90	15
23	16	3:7	2000	DMA	90	15
24	16	1:3	1500	THF	90	15
25	12	1:3	1500	THF	120	15
26	12	3:7	1500	THF	90	15
27	12	3:7	2000	DMA	120	5
28	16	3:7	1500	DMA	90	15
29	16	3:7	1500	THF	90	15

30	16	1:3	1500	THF	120	15
31	12	3:7	2000	DMA	90	15
32	12	1:3	1500	DMA	120	5
33	16	1:3	2000	DMA	90	5
34	16	3:7	2000	DMA	120	5
35	12	3:7	1500	DMA	90	15
36	16	1:3	1500	DMA	120	15
37	16	3:7	2000	DMA	120	15
38	12	1:3	1500	DMA	90	15
39	16	3:7	2000	THF	90	5
40	16	1:3	2000	THF	120	5
41	16	3:7	1500	THF	120	5
42	12	1:3	2000	THF	120	15
43	12	3:7	2000	DMA	120	15
44	12	1:3	2000	DMA	90	5
45	12	3:7	1500	DMA	120	5
46	12	1:3	2000	DMA	120	15
47	16	3:7	2000	THF	120	15
48	16	1:3	2000	DMA	120	5
49	12	1:3	2000	THF	90	5
50	16	1:3	1500	DMA	90	5
51	16	3:7	1500	THF	90	5
52	12	1:3	1500	DMA	120	15
53	12	3:7	1500	THF	90	5
54	12	3:7	1500	THF	120	5
55	12	1:3	1500	THF	90	5
56	16	1:3	2000	THF	120	15
57	12	1:3	2000	THF	90	15
58	16	1:3	2000	THF	90	5
59	12	1:3	2000	DMA	120	5
60	16	3:7	1500	THF	120	15
61	12	3:7	1500	THF	120	15

62	12	3:7	2000	THF	90	15
63	12	1:3	2000	THF	120	5
64	12	3:7	2000	THF	120	15

Appendix II: NREL Statement

Please note that the NREL developed chart (Figure 1, "Best Research-Cell Efficiencies") does not imply an endorsement by NREL, the Alliance for Sustainable Energy, LLC, the operator of NREL, or the U.S. Department of Energy.

References

[1] Katagiri, H., Jimbo, K., Yamada, S., Kamimura, T., Maw, W. S., Fukano, T., Ito, T., and Motohiro, T., 2008, "Enhanced Conversion Efficiencies of Cu $_2$ ZnSnS $_4$ -Based Thin Film Solar Cells by Using Preferential Etching Technique," Appl. Phys. Express, **1**, p. 041201.

[2] Todorov, T. K., Reuter, K. B., and Mitzi, D. B., 2010, "High-Efficiency Solar Cell with Earth-Abundant Liquid-Processed Absorber," Adv. Mater., **22**(20), pp. E156–E159.

[3] Binetti, S., Acciarri, M., Le Donne, A., Morgano, M., and Jestin, Y., 2013, "Key Success Factors and Future Perspective of Silicon-Based Solar Cells," Int. J. Photoenergy, **2013**, pp. 1–6.

[4] Jackson, P., Hariskos, D., Lotter, E., Paetel, S., Wuerz, R., Menner, R., Wischmann, W., and Powalla, M., 2011, "New World Record Efficiency for Cu(In,Ga)Se2 Thin-Film Solar Cells beyond 20%," Prog. Photovolt. Res. Appl., **19**(7), pp. 894–897.

[5] Chang, Y.-M., Liao, C.-Y., Lee, C.-C., Lin, S.-Y., Teng, N.-W., and Huei-Shuan Tan, P., 2019, "All Solution and Ambient Processable Organic Photovoltaic Modules Fabricated by Slot-Die Coating and Achieved a Certified 7.56% Power Conversion Efficiency," Sol. Energy Mater. Sol. Cells, **202**, p. 110064.

[6] Brabec, C. J., Gowrisanker, S., Halls, J. J. M., Laird, D., Jia, S., and Williams, S. P., 2010, "Polymer-Fullerene Bulk-Heterojunction Solar Cells," Adv. Mater., **22**(34), pp. 3839–3856.

[7] Galagan, Y., Fledderus, H., Gorter, H., 't Mannetje, H. H., Shanmugam, S., Mandamparambil, R., Bosman, J., Rubingh, J.-E. J. M., Teunissen, J.-P., Salem, A., de Vries, I. G., Andriessen, R., and Groen, W. A., 2015, "Roll-to-Roll Slot-Die Coated Organic Photovoltaic (OPV) Modules with High Geometrical Fill Factors," Energy Technol., **3**(8), pp. 834–842.

[8] Galagan, Y., de Vries, I. G., Langen, A. P., Andriessen, R., Verhees, W. J. H., Veenstra, S. C., and Kroon, J. M., 2011, "Technology Development for Roll-to-Roll Production of Organic Photovoltaics," Chem. Eng. Process. Process Intensif., **50**(5–6), pp. 454–461.

[9] Gambhir, A., Sandwell, P., and Nelson, J., 2016, "The Future Costs of OPV – A Bottom-up Model of Material and Manufacturing Costs with Uncertainty Analysis," Sol. Energy Mater. Sol. Cells, **156**, pp. 49–58.

[10] Antony, J., 2003, *Design of Experiments for Engineers and Scientists*, Elsevier, Jordan Hill, UNITED KINGDOM.

[11] Cyr, P., "10 - Fractional Factorial Designs in 2 Levels."

[12] Perrin, R., 2008, *Real World Project Management: Beyond Conventional Wisdom, Best Practices, and Project Methodologies*, John Wiley & Sons, Hoboken, N.J.

[13] Box, G. E. P., "Must We Randomize Our Experiment?" [Online]. Available: https://williamghunter.net/george-box-articles/must-we-randomize-our-experiment. [Accessed: 18-Dec-2019].

[14] Zhu, Y., Liu, J., Jiao, Z., Yang, L., Qiao, B., Song, D., Huang, Y., Xu, Z., Zhao, S., and Xu, X., 2018, "Improving the Charge Carrier Transport and Suppressing Recombination of Soluble Squaraine-Based Solar Cells via Parallel-Like Structure," Mater. Basel, **11**(5), p. 759.

[15] Zheng, C., "Efficient Organic Photovoltaic Cells Employing Squaraines and Their Aggregates: Experiment and Theory," p. 216.

[16] "5.3.3.10. Three-Level, Mixed-Level and Fractional Factorial Designs" [Online]. Available: https://www.itl.nist.gov/div898/handbook/pri/section3/pri33a.htm. [Accessed: 08-Jan-2020].

[17] Hinkelmann, K., and Kempthorne, O., 2007, *Design and Analysis of Experiments, Volume 1: Introduction to Experimental Design*, John Wiley & Sons, Incorporated, Newy York, UNITED STATES.

[18] Li, G., "Efficient Inverted Polymer Solar Cells," Appl Phys Lett, p. 4.

[19] Li, S.-S., Tu, K.-H., Lin, C.-C., Chen, C.-W., and Chhowalla, M., 2010, "Solution-Processable Graphene Oxide as an Efficient Hole Transport Layer in Polymer Solar Cells," ACS Nano, **4**(6), pp. 3169–3174.

[20] Shrotriya, V., Li, G., Yao, Y., Chu, C.-W., and Yang, Y., 2006, "Transition Metal Oxides as the Buffer Layer for Polymer Photovoltaic Cells," Appl. Phys. Lett., **88**(7), p. 073508.

[21] Nunzi, J.-M., 2002, "Organic Photovoltaic Materials and Devices," Comptes Rendus Phys., **3**(4), pp. 523–542.

[22] Günes, S., Neugebauer, H., and Sariciftci, N. S., 2007, "Conjugated Polymer-Based Organic Solar Cells," Chem. Rev., **107**(4), pp. 1324–1338.

[23] Su, Y.-W., Lan, S.-C., and Wei, K.-H., 2012, “Organic Photovoltaics,” Mater. Today, **15**(12), pp. 554–562.

[24] Grancini, G., Maiuri, M., Fazzi, D., Petrozza, A., Egelhaaf, H. -j, Brida, D., Cerullo, G., and Lanzani, G., 2013, “Hot Exciton Dissociation in Polymer Solar Cells,” Nat. Mater. Lond., **12**(1), pp. 29–33.

[25] Clarke, T. M., and Durrant, J. R., 2010, “Charge Photogeneration in Organic Solar Cells,” Chem. Rev., **110**(11), pp. 6736–6767.

[26] Schwenn, P. E., Gui, K., Zhang, Y., Burn, P. L., Meredith, P., and Powell, B. J., 2012, “Kinetics of Charge Transfer Processes in Organic Solar Cells: Implications for the Design of Acceptor Molecules,” Org. Electron., **13**(11), pp. 2538–2545.

[27] Rand, B. P., Burk, D. P., and Forrest, S. R., 2007, “Offset Energies at Organic Semiconductor Heterojunctions and Their Influence on the Open-Circuit Voltage of Thin-Film Solar Cells,” Phys. Rev. B, **75**(11), p. 115327.

[28] Yang, W., Yao, Y., Guo, P., Sun, H., and Luo, Y., 2018, “Optimum Driving Energy for Achieving Balanced Open-Circuit Voltage and Short-Circuit Current Density in Organic Bulk Heterojunction Solar Cells,” Phys. Chem. Chem. Phys., **20**(47), pp. 29866–29875.

[29] Wang, C., Li, C., Wang, G., Wang, C., Ma, P., Huang, L., Wen, S., Guo, W., Shen, L., and Ruan, S., 2018, “Employing Pentacene To Balance the Charge Transport in Inverted Organic Solar Cells,” J. Phys. Chem. C, **122**(30), pp. 17110–17117.

[30] Proctor, C. M., Albrecht, S., Kuik, M., Neher, D., and Nguyen, T.-Q., 2014, “Overcoming Geminate Recombination and Enhancing Extraction in Solution-Processed Small Molecule Solar Cells,” Adv. Energy Mater., **4**(10), p. 1400230.

[31] Zheng, C., “Spectral Properties of Squaraines and Their Aggregates, Targeted for Use in Bulk Hetero-Junction Solar Cells,” p. 121.

[32] Zheng, C., Bleier, D., Jalan, I., Pristash, S., Penmetcha, A. R., Hestand, N. J., Spano, F. C., Pierce, M. S., Cody, J. A., and Collison, C. J., 2016, “Phase Separation, Crystallinity and Monomer-Aggregate Population Control in Solution Processed Small Molecule Solar Cells,” Sol. Energy Mater. Sol. Cells, **157**, pp. 366–376.

[33] Zhang, P., Ling, Z., Chen, G., and Wei, B., 2018, “Influence of Thermal Annealing-Induced Molecular Aggregation on Film Properties and Photovoltaic Performance of Bulk

Heterojunction Solar Cells Based on a Squaraine Dye," Front. Mater. Sci., **12**(2), pp. 139–146.

[34] Zheng, C., Penmetcha, A. R., Cona, B., Spencer, S. D., Zhu, B., Heaphy, P., Cody, J. A., and Collison, C. J., 2015, "Contribution of Aggregate States and Energetic Disorder to a Squaraine System Targeted for Organic Photovoltaic Devices," Langmuir, **31**(28), pp. 7717–7726.

[35] Coffey, T., Seredinski, A., Poler, J. N., Patteson, C., Watts, W. H., Baptiste, K., Zheng, C., Cody, J., and Collison, C. J., 2019, "Nanoscale Characterization of Squaraine-Fullerene-Based Photovoltaic Active Layers by Atomic Force Microscopy Mechanical and Electrical Property Mapping," Thin Solid Films, **669**, pp. 120–132.

[36] Chen, G., Sasabe, H., Lu, W., Wang, X.-F., Kido, J., Hong, Z., and Yang, Y., 2013, "J-Aggregation of a Squaraine Dye and Its Application in Organic Photovoltaic Cells," J. Mater. Chem. C, **1**(40), p. 6547.

[37] Chen, G., Si, C., Zhang, P., Wei, B., Zhang, J., Hong, Z., Sasabe, H., and Kido, J., 2017, "The Effect of Processing Solvent Dependent Film Aggregation on the Photovoltaic Performance of Squaraine:PC71BM Bulk Heterojunction Solar Cells," Org. Electron., **51**, pp. 62–69.

[38] Spencer, S., Hu, H., Li, Q., Ahn, H.-Y., Qaddoura, M., Yao, S., Ioannidis, A., Belfield, K., and Collison, C. J., 2014, "Controlling *J* -Aggregate Formation for Increased Short-Circuit Current and Power Conversion Efficiency with a Squaraine Donor: Controlling *J* -Aggregate Formation," Prog. Photovolt. Res. Appl., **22**(4), pp. 488–493.

[39] Zheng, C., Jalan, I., Cost, P., Oliver, K., Gupta, A., Misture, S., Cody, J. A., and Collison, C. J., 2017, "Impact of Alkyl Chain Length on Small Molecule Crystallization and Nanomorphology in Squaraine-Based Solution Processed Solar Cells," J. Phys. Chem. C, **121**(14), pp. 7750–7760.

[40] Kakani, S. L., and Kakani, A., 2004, *Material Science*, New Age International Ltd, Daryaganj, INDIA.

[41] Peumans, P., 2003, "Small Molecular Weight Organic Thin-Film Photodetectors and Solar Cells," J. Appl. Phys., **93**(7), pp. 3693–3723.

[42] Comly, J., "Automation Of Solid/Powder Dispensing: Much Needed, but Cautiously Used!" [Online]. Available: https://www.ddw-online.com/enabling-technologies/p146749-

automation-of-solid/powder-dispensing:-much-neededbut-cautiously-used!.html. [Accessed: 03-May-2020].